Guest-Assisted and Guest-Inhibited Shell Closures Provide Differently Shaped Carceplexes and Hemicarceplexes[1,2]

Roger C. Helgeson, Kyungsoo Paek, Carolyn B. Knobler, Emily F. Maverick, and Donald J. Cram*

Contribution from the Department of Chemistry and Biochemistry, University of California at Los Angeles, Los Angeles, California 90095

Received January 22, 1996[⊗]

Abstract: The syntheses are reported of ten new carceplexes, hemicarceplexes, or their free hosts by coupling different or similar pairs of cavitands at their rims with four $O(CH_2)_nO$ or four *m*-$(OCH_2)_2C_6H_4$ bridging groups. Different combinations of seven different cavitands and five different bridging groups were involved in the shell closures, whose yields ranged from 50 to 1.8%. Seven of the new hosts have like northern and southern hemispheres, whereas three possess differently shaped hemispheres. The yield patterns are interpreted in terms of complexing guest preorganizing the reaction partners for shell closure, or the reaction partners complexing each other in nonproductive binding which inhibits shell closure. Crystal structures are reported for one new cavitand, one new caviplex, and three new hemicarceplexes. Comparisons of changes in ^{1}H NMR spectra of incarcerated guests in different hosts provide interesting correlations of chemical shifts with structure.

Introduction

Earlier papers in this series reported the preparations and correlations of structures with binding properties of carcerands and hemicarcerands of general structure **1**.[3] The primary starting materials in the syntheses were octols **2**,[4] bromination of which gave **3**[5] (Chart 1). These conformationally mobile compounds were rigidified by reacting the four proximate pairs of hydroxyl groups with 4 mol of $BrCH_2Cl$ to give (for example) cavitands **4** or **5**, **4** being converted to tetrol **6**.[6] Two tetrols such as **6** or **7** were then coupled with four bridging units of varying lengths, bulks, and rigidities to produce many carcerand or hemicarcerand systems. These systems possess structurally enforced inner phases that are longer in the polar than in the equatorial dimension.[3] The R groups ("feet") were chosen to confer solubility properties or to aid in characterization.

Scale molecular model (CPK) examinations of hosts such as **1** and **4**−**7** suggest that they should possess approximate C_4 axes, an expectation confirmed by many crystal structure determinations of both types of species.[3] The important structural feature common to these cavitand, carcerand, and hemicarcerand families is the conformational rigidity of the eight-membered rings that define the polar regions of the hosts.[5]

This paper reports the syntheses and characterizations of new cavitands **8**−**12** and carcerand and hemicarcerand systems **13**, **14**, **16**, **17**, and **19**−**24** from conformationally mobile octols, **2** and **3**. Hosts **13** and **14** possess polar regions based solely on the eight-membered rings originating in tetrol **7** and differ only

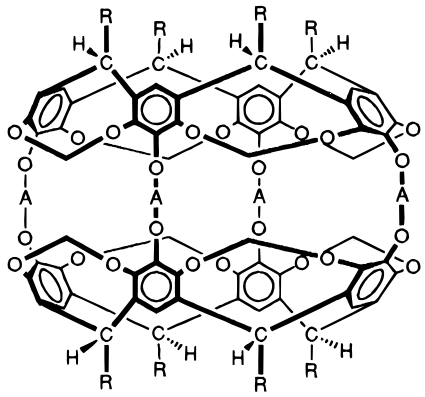

1 , R = $(CH_2)_4CH_3$ or CH_2CH_2Ph; A = $(CH_2)_n$
where n = 1, 4-6, or A = *o*-$CH_2C_6H_4CH_2$, etc.

in their equatorially-located aryl-connecting groups. Thus **13** possesses four OCH_2CH_2O aryl-connecting groups, and **14** possesses four $OCH_2CH_2CH_2O$ groups, completing the homologous series of host **1** in which A = $(CH_2)_n$ with $n = 1-6$.[6] The smallest member of this family of carcerands (**15b**, which is **1**, $n = 1$, R = CH_3) has been subjected to MM3 calculations, reported in a later section. In the following discussion, we will arbitrarily refer to the *intrahemispheric* groups (OCH_2O in **1**) that connect the aryls as *spanners*, and the *interhemispheric* groups (O−A−O) that connect the aryls as *bridges*.

Hosts **16** and **17** were composed by bridging two tetrol units of structure **9** with four $O(CH_2)_4O$ and four $O(CH_2)_5O$ units, respectively. In molecular models of **16** and **17**, the four *nine-membered rings* in each polar cap appear slightly more conformationally mobile than the *eight-membered rings* in **1**, **13**, **14**, and **15a**. Structure **18**, the same as **16** but with CH_3 feet, has also been subjected to MM3 calculations (see later section).

The four bridging groups in each of **19**−**24** are all *m*-$OCH_2C_6H_4CH_2O$ groups, which in CPK molecular models are long enough to bridge simultaneously polar caps of any of the pairs of the three tetrols, **6**, **9**, and **11**, and yet rigid enough to inhibit the passage of selected middle-sized guests of the right shape and size into and out of the inner phase of the hosts at

[⊗] Abstract published in *Advance ACS Abstracts,* May 15, 1996.

(1) Host−Guest Complexation. 66.

(2) We warmly thank the U.S. Public Health Service for a supporting grant (GM-12640) and Dr. Kurt L. Loening for nomenclature assistance.

(3) Cram, D. J.; Cram, J. M. In *Container Molecules and Their Guests*; Stoddart, J. F., Ed.; Monographs in Supramolecular Chemistry; The Royal Society of Chemistry: Cambridge, U.K., 1994; pp 131−216.

(4) Tunstad, L. M.; Tucker, J. A.; Dalcanale, E.; Weiser, J.; Bryant, J. A.; Sherman, J. C.; Helgeson, R. C.; Knobler, C. B.; Cram, D. J. *J. Org. Chem.* **1989**, *54*, 1305−1312.

(5) (a) Bryant, J. A.; Blanda, M. T.; Vincenti, M.; Cram, D. J. *J. Am. Chem. Soc.* **1991**, *113*, 2167−2172. (b) Cram, D. J.; Karbach, S.; Kim, H.-E.; Knobler, C. B.; Maverick, E. F.; Ericson, J. L.; Helgeson, R. C. *J. Am. Chem. Soc.* **1988**, *110*, 2229−2237.

(6) Cram, D. J.; Jaeger, R.; Deshayes, K. *J. Am. Chem. Soc.* **1993**, *115*, 10111−10116.

S0002-7863(96)00215-6 CCC: $12.00

Chart 1

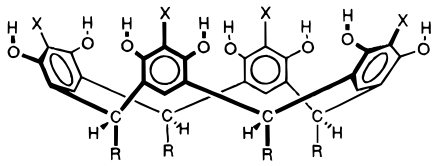

2, X = H, R = C_5H_{11} or CH_2CH_2Ph
3, X = Br, R = C_5H_{11} or CH_2CH_2Ph

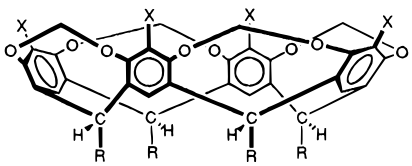

4, X = Br, R = C_5H_{11}
5, X = Br, R = CH_3
6, X = OH, R = C_5H_{11}
7 X,= OH, R = CH_2CH_2Ph

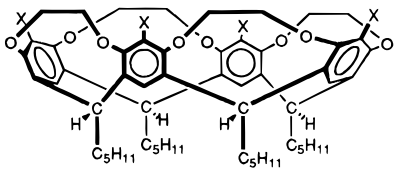

8, X = Br
9, X = OH

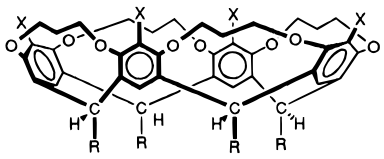

10, X = Br, R = C_5H_{11}
11, X = OH, R = C_5H_{11}
12, X = Br, R = CH_3

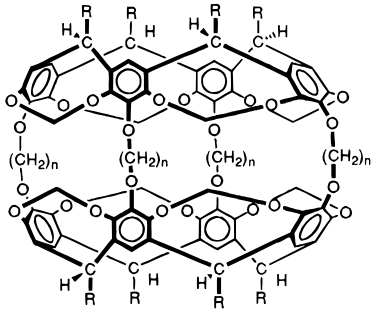

13, n = 2, R = CH_2CH_2Ph
14, n = 3, R = CH_2CH_2Ph
15a, n = 1, R = CH_2CH_2Ph
15b, n = 1, R = CH_3

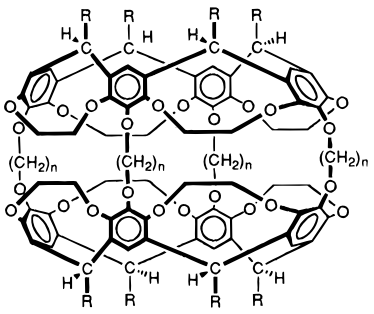

16, n = 4, R = C_5H_{11}
17, n = 5, R = C_5H_{11}
18, n = 4, R = CH_3

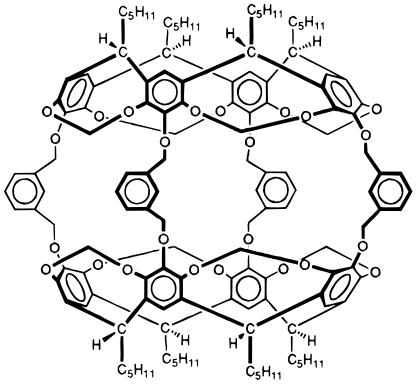

19

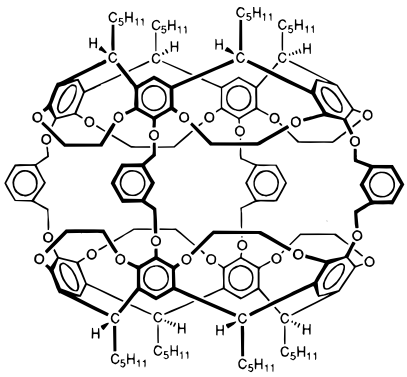

20

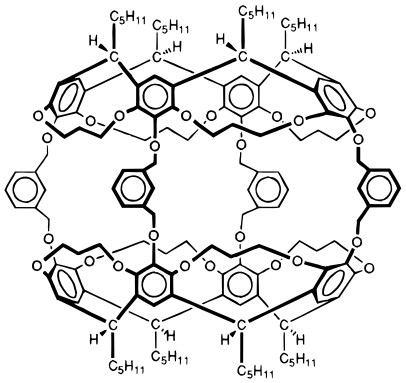

21

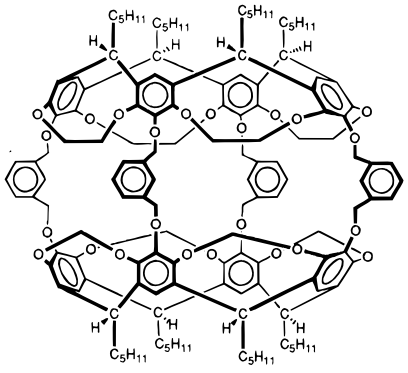

22

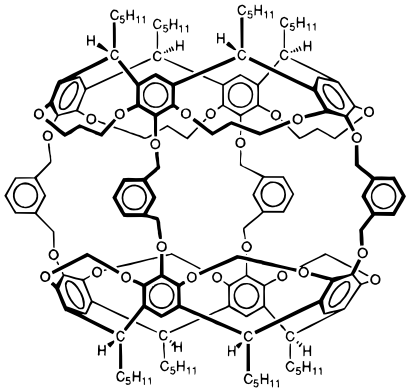

23

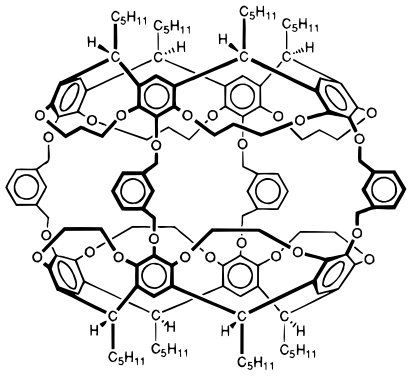

24

convenient temperatures. Of these hosts, **19**−**21** have the same northern and southern polar caps, whereas in **22**−**24** the polar caps are different. Thus **19** involves polar caps composed only of eight-membered rings, **20** involves polar caps containing only nine-membered rings, and **21** involves polar caps containing only ten-membered rings. Host **22** has one polar cap involving eight-membered rings and the other, nine-membered rings. Host **23** has one polar cap composed of eight-membered and the other of ten-membered rings. Host **24** has one polar cap composed of only nine- and the other of ten-membered rings.

Results and Discussion

Syntheses. Octol **2**, R = $(CH_2)_4CH_3$ (prepared as before from resorcinol and hexanal (71%)),[4] was brominated to give tetrabromide **3**, R = $(CH_2)_4CH_3$ (44%), which when treated with $BrCH_2Cl-Cs_2CO_3$ closed four eight-membered rings to provide **4** (56%), similar to the procedure used to prepare **5**.[5a] Aryl tetrabromide **4** was lithiated with BuLi in THF at −78 °C, and the resulting organometallic was boronated with $B(OCH_3)_3$ (−78 to 25 °C). Without isolation, the $[ArB(OCH_3)_2]_4$ intermediate

was oxidized at −78 °C with H_2O_2 to produce tetrol **6**[6] (63%). Tetrol **7** was also previously reported.[7a]

Similar procedures were used to prepare cavitands **8**−**12**. Treatment of octaphenolic tetrabromide **3**, R = $(CH_2)_4CH_3$, with $TsOCH_2CH_2OTs$[8] −DMSO[8]−K_2CO_3 closed four nine-membered rings to give tetrabromide **8** (46%), which was converted to tetrol **9** (61%) by the same method used to convert **4** to **6** (see above). Similarly **3**, R = $(CH_2)_4CH_3$, when mixed at ambient temperature with $TsOCH_2CH_2CH_2OTs$, closed four ten-membered rings to produce tetrabromide **10** (40%), which was oxidized to tetrol **11** (26%) by the same method applied to making **6** from **4**. Tetrabromide **12**, required for crystal structure determination, has been reported.[5b] These simple reactions made readily available the two key highly-preorganized new tetrols, **9** and **11** (**6** and **7** were in hand).

Carceplexes **13**⊙DMA[8,9] and **14**⊙DMA were prepared by treating tetrol **7**[7a] with $TsOCH_2CH_2OTs$ and $TsOCH_2CH_2CH_2OTs$ (respectively) at 60−100 °C in DMA at high dilution, the shell closures proceeding in 29% and 20% yields, respectively. These yields were the best obtained in three shell closures leading to each complex. Attempts to decomplex **14**⊙DMA by heating it to 215 °C for 72 h in 1,2,4-$Cl_3C_6H_3$ resulted in recovery of the intact complex. A complete summed elemental analysis of **13**⊙DMA was 99.99%, and of **14**⊙DMA was 99.93%, demonstrating that the carceplexes were 1:1 host:guest.

Carceplex **16**⊙DMSO[8] was synthesized in 9% yield (best obtained in five runs) from the expanded tetrol **9** and $TsO(CH_2)_4OTs$ at 74 °C in Cs_2CO_3−DMSO[8] at high dilution. Examination of CPK models of **16** shows the gaps between the polar caps to be much smaller than in carcerands based on tetrol **7** and the same equatorial $[O(CH_2)_4O]_4$ bridging units. The free hemicarcerand **17** was isolated in 7.5% yield (best obtained in four runs) when tetrol **9** was shell-closed with $TsO(CH_2)_5OTs$[8]−Cs_2CO_3−DMA.[8] It is very likely that **17**⊙DMA was formed in the reaction, and that the hemicarceplex decomplexed during the procedure used for isolation. Molecular model (CPK) examination of **17** and DMA suggests that there is little constraint to the passage of this guest through equatorially-located portals, and little *constrictive binding* in the complex.[10]

Repeated attempts (four) failed to shell-close 2 mol of tetrol **9** with 4 mol of $TsO(CH_2)_3OTs$ to form the analog of **14** but with expanded hemispheres. Models (CPK) of the target compounds are barely assemblable since the eight OCH_2CH_2O intrahemispheric spanning groups impinge pairwise on each others' space in the model. In tetrol **9** the four aryl planes are farther from one another at the rim of the bowl than the planes in **6** and **7**, requiring a longer bridge to hold two molecules of **9** rim-to-rim than two molecules of **6** or **7** (see Crystal Structures, below).

Carcerands **19**−**21** are composed of two like hemispheres linked to one another by four interhemispheric *m*-$OCH_2C_6H_4CH_2O$ *bridging groups*. The three hosts differ only in the lengths of the four $O(CH_2)_nO$ *spanners* that compose each hemisphere; $n = 1$ in **19**, $n = 2$ in **20**, and $n = 3$ in **21**. The respective tetrols **6**, **9**, and **11** when shell-closed in reactions with *m*-$ClCH_2C_6H_4CH_2Cl$−Cs_2CO_3−NMP[8] at 25−60 °C at moderate dilution provided **19** in 50% and **20** in 8% yield and **21** in nondetectable amounts. These yields were the best of three or more runs. Accordingly, the three tetrols were treated with large excesses (see Experimental section) of the above reactants, which provided **25**, **26**, and **27** in 60, 69, and 63% yields, respectively. The resulting tetrachlorides were fully characterized. The expectation was that fewer side reactions would be encountered in shell closures involving the sequential making of the four bonds leading to **19**−**24** in reactions between **25**−**27** and tetrols **6**, **9**, and **11** than in the making of eight bonds sequentially leading to the same corresponding products. Scheme 1 outlines the results obtained under a standard set of conditions, with NMP[8] as solvent, a temperature of 25 → 60 °C and Cs_2CO_3 as base. The yields quoted are the highest obtained in three to five runs and are not far from the lowest yields. Generally the reactions that gave the lowest yields were run the most times.

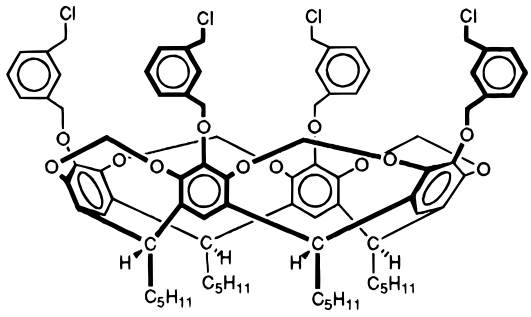

25

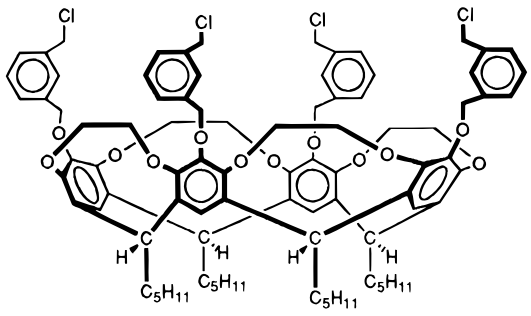

26

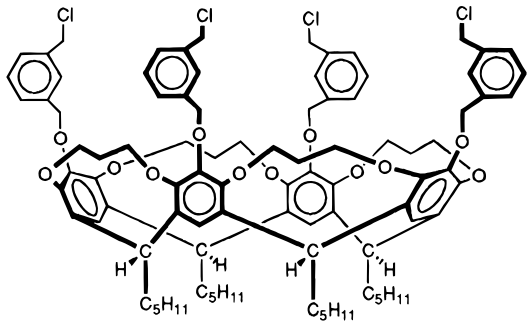

27

Inspection of the yields observed when **19**−**24** were prepared by two different methods reveals startling differences (see Scheme 1).Preparation of **19** from 2 mol of **6** and 4 mol of *m*-$ClCH_2C_6H_4CH_2Cl$ gave a 50% yield (eight bonds made), which was 23 times higher than when **6** reacted with **25** (four bonds made). We suggest that NMP might have templated the

(7) (a) Sherman, J. C.; Cram, D. J. *J. Am. Chem. Soc.* **1989**, *111*, 4527−4528. (b) Sherman, J. C.; Knobler, C. B.; Cram, D. J. *J. Am. Chem. Soc.* **1991**, *113*, 2194−2204. (c) Robbins, T. A.; Knobler, C. B.; Bellew, D. R.; Cram, D. J. *J. Am. Chem. Soc.* **1994**, *116*, 111−122. (d) Byun, Y.-S.; Robbins, T. A.; Knobler, C. B.; Cram, D. J. *J. Chem. Soc., Chem. Commun.* **1995**, 1947−1948.

(8) DMA stands for *N*,*N*-dimethylacetamide; DMF for dimethylformamide; NMP for *N*-methylpyrrolidinone; DMSO for dimethyl sulfoxide; THF for tetrahydrofuran; and Ts for *p*-tolylsulfonyl.

(9) We suggest the use of the symbol ⊙ to indicate an incarcerated complex and the symbol ∪ for the nesting complex found in the caviplexes. These are modifications of a dot alone between two molecules, which has been used to indicate crystalline interstitial solvates. Sometimes all three of these phenomena are found in a single crystalline complex and require differentiation.

(10) Cram, D. J.; Blanda, M. T.; Paek, K.; Knobler, C. B. *J. Am. Chem. Soc.* **1992**, *114*, 7765−7773.

Scheme 1. Shell-Closure Yields as Structures of Cavitands Vary

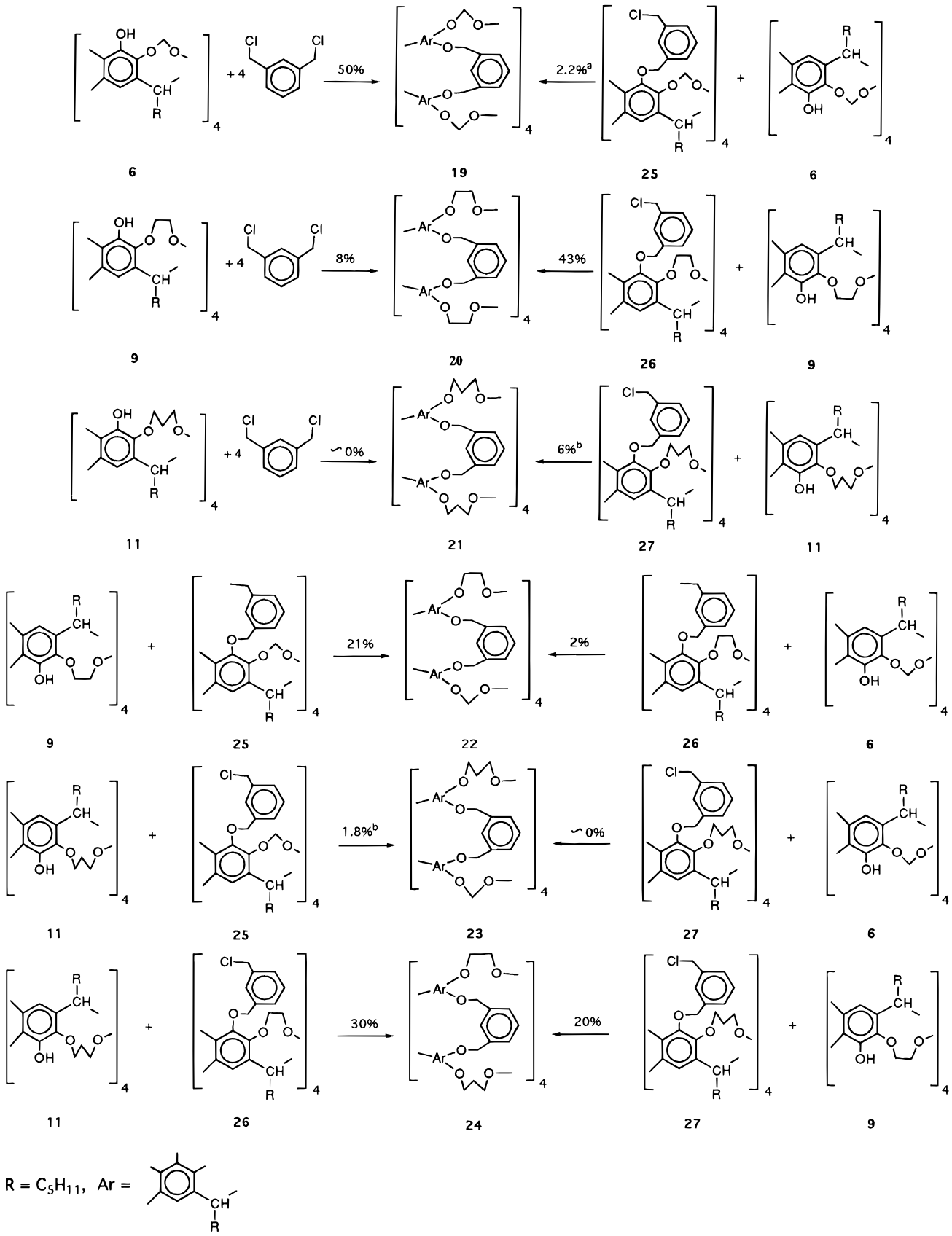

[a] 1,2,3-$(CH_3O)_3C_6H_3$ when present in the NMP solvent (5% w:w) had no effect on the yield. [b] 1,2,3-$(CH_3O)_3C_6H_3$ had to be present (5% w:w) in the NMP solvent before any shell-closed product was detectable.

introduction of the first two bridges in the product-determining steps when **6** and *m*-$ClCH_2C_6H_4CH_2Cl$ were starting materials. We previously explained the 40−60% yields of **1**⊙Guest (R = CH_2CH_2Ph, A = CH_2) from tetrol **7** and $BrCH_2Cl-Cs_2CO_3$[7a,b] by templation of the shell closure by DMA, DMF, or DMSO. Subsequently, Sherman et al. beautifully confirmed this hypothesis by correlating tetrol cavitand dimerization with cavitand guest binding power and yields of carceplexes.[11] In CPK molecular models of mono- or dibridged intermediates, the remaining four or six hydroxyl functional groups keep the two

bowls preorganized for shell closure. It is highly likely that **19**⊙NMP is the initial shell-closed product, which dissociates during isolation. In the reaction of **6** with **25**, hydrogen bonding of **6** with itself probably inhibits shell closure and directs the reaction toward formation of oligomers.

In the production of **20**, the yield from **26** and **9** at 43% was a factor of 5 higher than the yield obtained from **9** and *m*-$ClCH_2C_6H_4CH_2Cl$ at 8%. Models (CPK) of tetrol **9** dimer based on the crystal structure of **9**∪$(CH_3)_2CO$ (see later section) are poorly preorganized for the simultaneous 4-fold hydrogen bonding which predisposes tetrol **6** to shell-close. A four-bond-making process with **26** and **9** as reactants is expected on a statistical basis to give a better yield than the eight-bond-making sequence required with **9** and *m*-$ClCH_2C_6H_4CH_2Cl$ in the absence of templating effects.

The synthesis of **21** from **27** and **11** in 6% yield is higher by a large but unavailable factor than the ≈0% yield from **11** and *m*-$ClCH_2C_6H_4CH_2Cl$. Model examination of the tetrol dimer of **11** (guided by the crystal structure of tetrabromide **12**, see later section) shows an even lower probability of being preorganized for shell closure by hydrogen bonding than the tetrol dimer of **9**. The reaction of **27** with **11** gave no detectable **21** when 1,2,3-$(CH_3O)_3C_6H_3$ was absent, but when present at 5% (w:w), the 6% yield was of the free host **21**. Probably the shell closure was templated, but the tris-ether guest escaped during isolation. Models of **21** in the proper conformation allow models of the guest to be readily inserted into and removed from the interior of **21**.

Carcerands **22**−**24** contain unlike northern and southern hemispheres. The synthesis of each of them was approached two different ways making use of different combinations of one tetrol (**6**, **9**, or **11**) and one tetrachloride (**25**, **26**, or **27**) as starting materials. The same standard conditions were used for these coupling reactions as were employed in the synthesis of the like-ended carcerands **19**−**21** (NMP[8] as solvent at medium dilution, 25 → 60 °C). Scheme 1 outlines the results of the six reactions involved. Tetrol **9** coupled with tetrachloride **25** gave a 21% yield of **22**, a factor of 10 larger than the 2% yield from tetrol **6** and tetrachloride **26**. The latter yield resembles that obtained when **6** reacted with tetrachloride **25** to give **19**. In both cases, the shell closure probably had to break up the dimer of **6**, whose reactions with **25** and **26** were predisposed to give non-shell-closed oligomers.

The projected synthesis of hemicarcerand **23** from tetrol **6** and tetrachloride **27** in practice failed to produce a detectable amount of **23**. The use of tetrol **11** and tetrachloride **25** gave 1.8% of **23**⊙1,2,3-$(CH_3O)_3C_6H_3$ when run in NMP containing the guest. Clearly, this tris-ether templated what shell closure occurred. Carcerand **23** contains two badly mismatched hemispheres, composed by 4-fold bridging of a cavitand rim of 24 members and a C_4 symmetry element with a cavitand rim of 32 members and only a near C_2 symmetry element. In CPK models, the four $O(CH_2)_3O$ spanner groups in **23** have to adopt conformations different from the cavitand containing those groups as a condition of being coupled.

When the sizes of the two rims of the cavitands being coupled in carcerand formation are closer to one another, as in the two syntheses of **24**, the yields improve. Thus tetrol **11** with a 32-membered rim combines with tetrachloride **26** with a 28-membered rim to give hemicarcerand **24** in 30% yield. Similarly tetrol **9** with a 28-membered rim couples with tetrachloride **27** to provide **24** in 20% yield. The unsurprising generalization that best correlates yield with structure is as follows: *The shell closures involving starting materials that are the most conformationally preorganized for hemicarceplex formation provide the highest yields.*

In the shell closures of Scheme 1 leading to **19**−**24**, NMP probably occupies the interior of the hemicarcerands **19**, **20**, **22**, and **24**, but departs, during isolation, through the portals located in the equatorial region of the globes. These portals are composed of the following ring sizes: **19**, 28-membered; **20**, 30-membered; **21**, 32-membered; **22**, 29-membered; **23**, 30-membered; and **24**, 31-membered. In CPK models made with new bonds and after many trials, NMP can be manipulated into these hemicarcerand interiors without breaking any bonds. In the synthesis of **21** from **27** and **11**, and of **23** from **25** and **11**, no shell closure occurred unless the NMP solvent contained 1,2,3-$(CH_3O)_3C_6H_3$ (5%, w:w). This "catalysis" of the reactions leading in shell closure to **21** strongly suggests that 1,2,3-$(CH_3O)_3C_6H_3$ templates the product-determining step, but undergoes a mass-law-driven exchange with NMP as guest before or after the final bridge or bridges are in place. Otherwise **21**⊙1,2,3-$(CH_3O)_3C_6H_3$ would have been the product isolated, just as **23**⊙1,2,3-$(CH_3O)_3C_6H_3$ was isolated as the product of templation.

Hypotheses Derived from CPK Model Examinations of the Hemicarcerands of Scheme 1

Comparisons of models of **19**−**24** suggest the following interesting hypotheses.

1. Although cavitands **9** and particularly **12** (a model for **11**) have crystal structures far from possessing C_4 axes (see next section), assembly of them into carcerands such as **19**−**24** requires them to conformationally reorganize toward structures having C_4 axes.

2. Of the three hemicarcerands possessing like hemispheres, the more the starting two molecules of cavitand must conformationally reorganize to meet the geometric requirements for the 4-fold bridging reactions to occur, the lower the yields are likely to be. Of the three tetrols **6**, **9**, and **11**, **11** must reorganize the most to shell-close. The product **21** is formed in the lowest of the six yields.

3. The two simplest conformations of **21** which possess C_4 axes are (a) that in which the four bridges are outward (bo) and the spanners inward (si) and (b) that in which the four bridges are inward (bi) and the spanners are outward (so). The bo-si conformation has a relatively short polar axis, long equatorial axes, and essentially no portals. The bi-so conformation has a relatively long polar axis, short equatorial axes, and large portals.

4. In **23** the two kinds of hemispheres best match one another for occurrence of their bridging reactions when the northern hemisphere with $[O(CH_2)_3O]_4$ spanners assumes the bi-so conformation.

5. The six hemicarcerands in those conformations which maximize their portal sizes assume the following order with respect to decreasing portal size: **21** > **23** > **19** > **24** > **22** > **20**. However, the portal adaptability to guest shape for complexation−decomplexation assumes the order **21** > **23** > **24** > **19** > **20** > **22**.

6. The six hemicarcerands in those conformations that maximize their inner volume have the order **21** > **24** > **20** > **23** > **22** > **19**. No conformations are available that collapse the cavity.

Crystal Structures

Crystal structures were determined for caviplex **9**∪$(CH_3)_2CO{\cdot}(CH_3)_2CO{\cdot}2H_2O$[9] and cavitand **12**, which when combined with that for the already-reported caviplex **5**∪$CHCl_3$[5b,9] provide a basis for comparisons of the effects of cavitand aryl spanner

(11) (a) Chapman, R. G.; Chopra, N.; Cochien, E. D.; Sherman, J. C. *J. Am. Chem. Soc.* **1994**, *116*, 369−370. (b) Chapman, R. G.; Sherman, J. C. *J. Am. Chem. Soc.* **1995**, *117*, 9081−9082. (c) Fraser, J. R.; Borecka, B.; Trotter, J.; Sherman, J. C. *J. Org. Chem.* **1995**, *60*, 1207−1213.

lengths on the shapes of bowl-type hosts.[5b] Crystal structures were also determined for the new carceplexes **14**⊙NMP∪2PhNO$_2$[9] and **14**⊙DMA∪2CHCl$_3$·6CHCl$_3$, based on cavitand **7**, and for carceplex **16**⊙DMSO∪2PhNO$_2$ based on cavitand **9**. Chart 2 provides side and face stereoviews of the three cavitands. Feet are omitted from the face views. Also shown are side stereoviews of the three new carceplexes, and stereoviews of the inner phases of the hemicarceplexes, including only the guest and the bridges themselves.

The three cavitands **5**, **9**, and **12** are generally conical, the base of the cone being composed of four methine carbons which are close to square planar. Attached to these methines are the four feet, whose character has little effect on the cavity shape.[3] The distances and angles relevant to the shapes of the cavities are listed in Table 1 and defined in the general drawing **28**. Since the carcerands' two hemispheres are composed of two of the same kinds of cavitands attached to one another at their rims, the same distances and bond angles used to define the cavitands' cavities can also be employed to define those of the two polar regions of the three carceplexes **14**⊙NMP, **14**⊙DMA, and **16**⊙DMSO. Since each carcerand (not their guests) has a center of symmetry, the parameters for the northern and southern polar caps are the same, and only one set need be listed in Table 1. Comparison of the values of the parameters addresses such questions as how the cavities of the cavitands change as the lengths of the O(CH$_2$)$_n$O spanners change, and how much such changes carry over into the carcerands. A comparison of the parameters for **14**⊙NMP and **14**⊙DMA provides a measure of guest-structural effect on the host. The effects of changes in shape of the polar regions on the dispositions of the bridges in the carceplexes are discussed in the next section.

The differences in the lengths of the two diagonal distances between the top aryl carbons (plane *a* of **28**) measure how much the cavities depart from having a C_4 axis. The two distances in **5**, **14**⊙NMP, and **14**⊙DMA (OCH$_2$O spanners) average 7.92 ± 0.09, 8.02 ± 0, and 7.88 ± 0.12 Å, respectively. Thus the maximum deviation of the tops of these cavities from having a C_4 axis is 1.5%. The averages of the diagonals (plane *b* of **28**) at the bottoms of the cavities are respectively 5.24 ± 0.01, 5.18 ± 0.03, and 5.24 ± 0.04 Å for the same three systems. By this measure the deviation of these cavities from having a C_4 axis is not significant. For both planes *a* and *b*, the deviation is greater between **14**⊙NMP and **14**⊙DMA than between cavitand **5** and the two carcerands. The carbon atoms' maximum out-of-plane distance from the least-squares planes *a*, *b*, and *c* (see **28**) for these three systems is also very small, reaching a maximum in **5** of ± 0.08 Å. Similarly, for these three molecules, the angles α (12 measurements) between the planes of the benzene rings and planes *a* varied little, the overall α_{av} and its maximum deviation being 60.8° ± 1.4°, or 2.3%. As concluded from CPK model examination, the cavity in which the spanning groups are OCH$_2$O is too rigid to vary much from host to host.

Comparisons of the difference in lengths of the two diagonal distances (plane *a* of **28**) provide an interesting answer to the important question of whether the narrowness of the cavity of cavitand **9** carries over during shell closure to the hemispheric parts of the cavity of **16**. This difference for **9** is 1.47 Å, which decreases to 0.75 Å in **16**, which should substantially open the cavity of **16** to many more guest moieties, for example methyl or methoxyl groups, than might be complementary in shape to **9**.

When the cavitand spanners become OCH$_2$CH$_2$O as in **9** and **16**, the cavity shapes lose their virtual C_4 symmetry by widening in one dimension and narrowing in a second. The resulting roughly rectangular shape of the top of the cavity of **9** is visible in the face stereoview of the caviplex of **9** in Chart 2. The two diagonals in plane *a* (see **28**) for **9** are 7.87 and 9.34 Å in length to provide a $(C\cdots C)_{av}$ of 8.60 ± 0.74 Å or an 8.6% deviation from C_4 symmetry. This deviation is less in the polar caps of **16** at $(C\cdots C)_{av}$ = 8.60 ± 0.38, or 4.4% deviation from C_4 symmetry. The maximum out-of-plane *a* distance of any of the four carbons is 0.26 Å for **9** and 0.10 Å in **16**. The maximum out-of-plane *b* distance is only 0.03 Å for **9** and 0.04 Å for **16**, the geometry of plane *b* being relatively insensitive to the lengths of the spanning groups. The α_{av} values (see **28**) are the most sensitive to this parameter, changing from 61.2° ± 1.6° for **5** with OCH$_2$O spanners to 50.5° ± 10.0° for **9** and 51.4° ± 8.1° for **16** with OCH$_2$CH$_2$O spanners.

Increasing the length of the cavitand spanners to that of OCH$_2$CH$_2$CH$_2$O as in **12**, combined with its conformation with two spanners inward (si) and two spanners outward (so), makes the cavity too narrow and too shallow to accommodate ordinary solvent guests. No guest was found in **12**. The reluctance of **12** to include solvent suggests that solvent may be unable to template shell closures, which would account for our inability to obtain **21** from tetrol **11** and *m*-ClCH$_2$C$_6$H$_4$CH$_2$Cl (Scheme 1). In **12** the values of the diagonal lengths in plane *a* become 10.39 and 4.80 Å to give 7.60 ± 2.80 Å, or a 37% deviation from C_4 symmetry. The maximum out-of-plane *a* distance increases to 1.12 Å, but as with **5** and **9** the C···C diagonal lengths for plane *b* vary very little at 5.26 ± 0.22 Å. Also the maximum out-of-plane *b* distance is only 0.07 Å. In contrast, α_{av} = 50.1° ± 26°.

An impression of the variation of the cavity depths with changes in cavitand spanner lengths is gained from the distance *d* from least-squares plane *b* to plane *a*. In **5**, **14**⊙NMP, and **14**⊙DMA, with OCH$_2$O spanners, these values are 2.44, 2.40, and 2.45 Å, respectively. For **9** and **16**⊙DMSO with OCH$_2$CH$_2$O spanners, *d* values are 2.12 and 2.16 Å, respectively. For **12** with OCH$_2$CH$_2$CH$_2$O spanners, *d* = 1.95 Å. As expected, the cavities become shallower as the spanners become longer.

Comparisons of MM3 Energy-Minimized Calculated Structures of Carcerands and Carceplexes with Crystal Structures of Analogous Compounds

We report here the results of comparisons between a starting model, crystal structure **15a**⊙DMF with CH$_2$CH$_2$Ph feet replaced by CH$_3$, and MM3 energy-minimized, calculated structures of **15b**, **15b**⊙DMF, and **15b**⊙DMA. These hosts possess the smallest spanners and bridges, all 12 of which are OCH$_2$O. Likewise, comparisons are made between a starting model, crystal structure **16**⊙DMSO with C$_5$H$_{11}$ feet replaced by CH$_3$, and calculated structures **18** and **18**⊙DMSO. Host **16** was chosen for these comparisons because its bridges [O(CH$_2$)$_4$O] are the shortest that have been preparable with (OCH$_2$CH$_2$O)$_4$ spanners. The reasonable assumption is made that the dimensions and shapes of the closed shells of the host are independent of the nature of the hydrocarbon feet (CH$_3$, C$_5$H$_{11}$, or CH$_2$CH$_2$Ph).[12] Hydrogen atoms for the crystal structure starting models are included in calculated positions (C−H distance 1.08 Å). Table 2 provides those structural and energy features chosen for comparisons that involve **15a** and **15b**, and Table 3 those that involve **16** and **18**. Although much of the strain in **15** and **16** is found in the deformed C$_{Ar}$−O−CH$_2$, O−CH$_2$−O, and O−CH$_2$CH$_2$−O bond angles, of more interest are the shapes, energies, and surfaces of these hosts. The parameters are as follows: (1) when present, the twist angle of one hemisphere

(12) In CPK models and numerous crystal structures already published (ref 3), the hemispheric parts of the structures of cavitands and carcerands and their complexes based on resorcinol are essentially independent of whether the four feet are CH$_3$, (CH$_2$)$_4$CH$_3$, or CH$_2$CH$_2$Ph.

Chart 2. Stereoviews of Crystal Structures

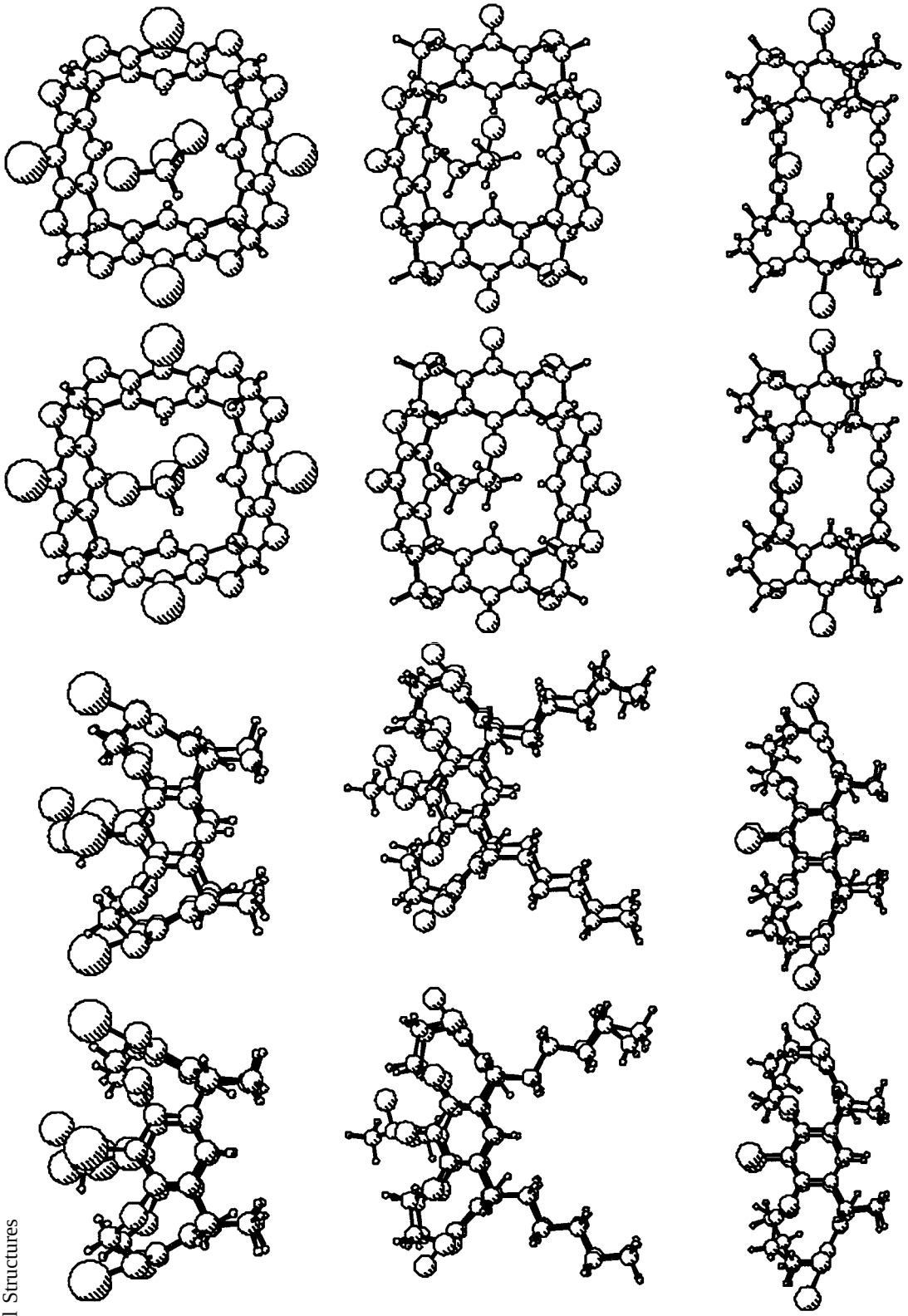

Chart 2. Stereoviews of Crystal Structures (continued)

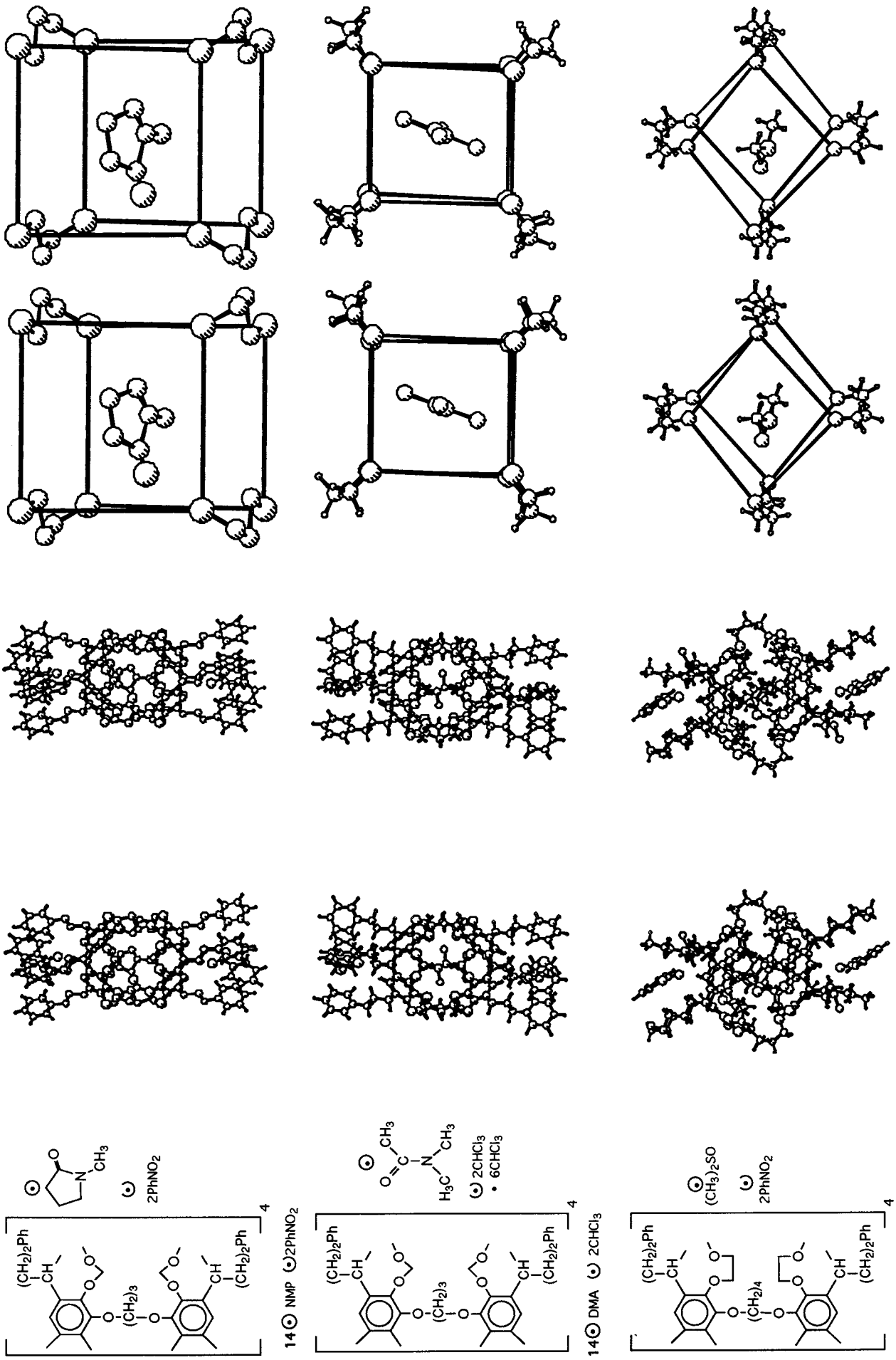

Table 1. Distances and Angles Relevant to Cavities of Hosts from Crystal Structures[a]

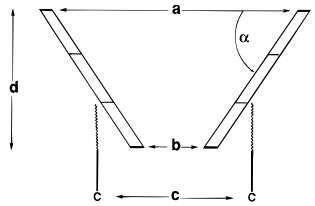

28

	5[b]	**9**	**12**	**14**⊙NMP	**14**⊙DMA	**16**⊙DMSO
			Distances (Å)			
C···C diagonals of plane *a* (*a*)	8.00, 7.83	7.87, 9.34	10.39, 4.80	8.02, 8.02	7.76, 7.99	8.22, 8.97
$(C\cdots C)_{av}$ for *a*	7.92	8.60	7.60	8.02	7.88	8.60
C···C diagonal difference	0.17	1.47	5.59	0.00	0.23	0.75
C out-of-plane *a*[c]	±0.02	±0.26	±1.12	±0.01	±0.05	±0.10
C···C diagonals of plane *b* (*b*)	5.25, 5.23	5.13, 5.08	5.48, 5.05	5.16, 5.21	5.27, 5.20	5.13, 5.10
$(C\cdots C)_{av}$ for *b*	5.24	5.10	5.26	5.18	5.24	5.12
C out-of-plane *b*[c]	±0.02	±0.03	±0.07	±0.01	±0.02	±0.04
C···C diagonals of plane *c* (*c*)	7.34, 7.02	7.17, 7.24	7.38, 7.38	7.16, 7.22	7.19, 7.25	7.21, 7.21
$(C\cdots C)_{av}$ for *c*	7.18	7.20	7.38	7.19	7.22	7.21
C out-of-plane *c*[c]	±0.08	±0.01	±0.00	±0.05	±0.06	±0.01
plane *a* to plane *b* (*d*)[d]	2.44	2.12	1.95	2.40	2.45	2.16
			Angles (deg)			
between planes of benzenes and *a* (α)	60.9, 62.8, 59.9, 61.0	41.1, 61.0, 40.9, 58.9	26.5, 70.9, 26.5, 76.6	59.3, 59.7, 59.8, 59.0	60.8, 63.2, 60.7, 62.4	48.2, 52.6, 45.1, 59.5
α_{av}[c]	61.2 ± 1.6	50.5 ± 10	50.1 ± 26	59.4 ± 0.4	61.8 ± 1.4	51.4 ± 8.1

[a] *a*, *b*, and *c* are least-squares planes of four atoms each, defined in diagram **28**. [b] Values taken from ref 5b. [c] ± values are maxima, not averages. [d] Average of distances of atoms in plane *a* from least-squares plane *b*.

Table 2. Structural Parameters of Crystal Structure of **15a**⊙DMF and MM3 Energy-Minimized Structures of **15b**, **15b**⊙DMF, and **15b**⊙DMA

internal coordinate	A cryst struct, **15a**⊙DMF[a]	MM3 B **15b**⊙DMF	MM3 C **15b**	MM3 D **15b**⊙DMA
$C_{Ar}C_{Ar}C_{Ar}C_{Ar}$ planes[b]				
twist (deg)	18	19	19	19
dist (Å)	4.0	4.0	4.0	4.0
steric energy,[d] MM3 (kcal mol^{-1})	>300[c]	149	160	155
host−guest van der Waals energy, (OPEC)[e] (kcal mol^{-1})	−6[c]	−22.3		−23.8
"free area" of host (Å^2)	501	521	520	520
free area of host *with guest present* (Å^2)	480[c]	501		492

[a] The starting structure for calculations is **15a**⊙DMF, with CH_2CH_2Ph feet replaced by CH_3. [b] These are the least-squares planes defined by the four aryl carbons attached to the ends of the four interhemispheric bridging groups [$(OCH_2O)_4$]; planes *a* in **28**. [c] Values are not meaningful because DMF is disordered and poorly described. [d] See ref 13a. [e] See ref 13b.

with respect to the other; (2) when present, the displacement distance or shift of one hemisphere with respect to the other; (3) the distance between the aryl carbon planes that describe the effective length of the bridges; (4) when not equal, the distance between the pairs of oxygens that terminate the bridges; (5) the MM3-calculated[13a] steric energies of the free hosts and complexes; (6) the host−guest van der Waals energies;[13b] and (7) the "free areas" [13b] of the carcerands, uncomplexed and complexed. The "free area" is the sum of the surface areas of the atoms in the host molecule (calculated at van der Waals radius plus 0.2 Å) that are not in contact with or penetrated by the surfaces of other atoms. It is the area that is "free" to contact solvent or guest. Thus in Tables 2 and 3 each guest reduces the "free area" of its host by an amount that is a measure of host−guest interaction. These surface area calculations were made using the computer program OPEC,[13b] which in the past has been applied to calculating changes in occupied and nonoccupied areas of other host-guest systems.[14]

The crystal structure conformations of the bridges in **15a**⊙DMF[15] are not far from the calculated minimized values of **15b**⊙DMF, empty **15b**, or **15b**⊙DMA (parameters are omitted from Table 2). Thus the host as found in the crystal and in its idealized MM3 form is apparently quite rigid, and it changes very little geometrically upon inclusion of either guest. The bridge CH_2 groups turn *outward* in both the crystal structures[3] and calculated structures. Both CPK models and MM3 calculations indicate that the energy of *empty* **15** is lower with the bridge CH_2 groups turned *inward*. However, empty **15** has never been isolated; the carceplexes of **15** cannot be decomplexed.

Notice in Table 2 that the calculated steric energy of the empty host is 11 kcal higher than that for MM3-minimized **15b**⊙DMF and 5 kcal higher than that for **15b**⊙DMA in the calculated models. Thus the presence of guests in host reduces the steric energy by 5−11 kcal mol^{-1}. Of the two guests, DMA fits much more tightly into **15b** than DMF. This conclusion, very obvious from CPK model constructions, is reflected in the reduced "free surface area" for **15b**⊙DMA of 28 Å^2 (column D) as compared to that for **15b**⊙DMF of 20 Å^2 (column B).

(13) (a) Allinger, N. L.; Yuh, Y. H.; Lii, J.-H. *J. Am. Chem. Soc.* **1989**, *111*, 8551−8566. (b) Gavezzotti, A. *J. Am. Chem. Soc.* **1985**, *107*, 962−967.

(14) Choi, H.-J.; Cram, D. J.; Knobler, C. B.; Maverick, E. F. *Pure Appl. Chem.* **1993**, *66*, 539−543.

(15) Crystal structures for **15a**⊙DMF refined to $R = 0.13$ and **15a**⊙DMSO refined to $R = 0.15$ have been determined and will be published elsewhere by C. B. Knobler, E. F. Maverick, and D. J. Cram.

Table 3. Structural Parameters of Crystal Structure of **16**⊙DMSO, and MM3 Energy-Minimized Structures of **18** and **18**⊙DMSO with Varied Bowl Organizations

		MM3			
internal coordinate	A cryst struct, **16**⊙DMSO[a]	B **18**⊙DMSO	C host only, **18**	D bowls 2m,[b] **18**⊙DMSO	E bowls ~ C_2, **18**⊙DMSO
O···O dist (Å)					
long bridge	4.38	4.50	4.48	4.50	4.41
short bridge	3.62	3.73	3.72	3.49	3.63
C_{Ar}−O−C angles (deg)					
long bridge	119, 110	123, 116	123, 116	120, 116	122, 114
short bridge	116, 114	119, 117	118, 117	117, 116	120, 118
$C_{Ar}C_{Ar}C_{Ar}C_{Ar}$ planes[c] (Å)					
shift[d]	1.33	1.32	1.29	1.13	1.28
dist	5.96	6.05	6.05	5.87	5.92
diagonals	8.97, 8.22	9.13, 8.40	9.11, 8.37	9.29, 8.42	9.11, 8.54
steric energy,[e] MM3 (kcal mol^{-1})	300	149	166	152	159
host−guest interact. energy, (OPEC)[f] (kcal mol^{-1})	−18.6	−18.8		−19.0	−19.0
"free area" of host (Å^2)	703	744	743	740	733
free area of host *with guest present* (Å^2)	696	739		735	728

[a] The starting structure for calculations is **16**⊙DMSO, with CH_2CH_2Ph feet replaced by CH_3. [b] Bowls 2m means bowls contain two (approximate) mirror planes perpendicular to one another. [c] The least-squares planes defined by the four aryl carbons attached to each end of the four interhemispheric bridging groups [$(O(CH_2)_4O)_4$]; planes *a* in **28**. [d] Calculated from the distance between centroids of the parallel least-squares planes. [e] Reference 13a. [f] Reference 13b.

The very tight fit of DMA in the cavity of **15** may be the reason for the non-symmetric structure of **15a**⊙DMA,[7b] in which two of the bridges have an intermediate conformation, partially turned along the surface of the globe.

The host−guest van der Waals energy[13b] calculated for MM3-minimized **15b**⊙DMF is −22.3 kcal mol^{-1} (column B) and for **15b**⊙DMA is −23.8 kcal mol^{-1} (column D). Thus the host−guest energy for **15b**⊙DMA is 1.5 kcal mol^{-1} more stabilizing than that for **15b**⊙DMF. This fact correlates with the calculated 8 Å^2 greater surface area common to host and guest in **15b**⊙DMA compared to that in **15b**⊙DMF. These high energies indicating strong host−guest attractions include some close contacts (repulsive in these force fields), for example, a host C−H···O guest contact of only 2.21 Å in **15b**⊙DMA.

Table 3 combines the results of the crystal structure determination of **16**⊙DMSO with MM3-minimized structures of **18**, which is the same as **16** except with CH_3 rather than $(CH_2)_4$-CH_3 feet.[12] Column A (Table 3) provides the host's crystal structure parameters, B, those of the crystal structure minimized with MM3, and C, those of the MM3-minimized crystal structure with the DMSO guest absent. An important complicating feature of the host structure compared to that of **14** or **15** is that the $O(CH_2)_4O$ bridges connecting the two bowls must span two different kinds of distances, two between the *upward-tilting* aryls (short bridges) and two between the *outward-tilting* aryls (long bridges). The center of symmetry for the host in the crystal makes the two bowls equivalent to one another, but the bridges have different C_{Ar}−O−C angles for *upward-* and *outward-tilting* aryls. These four C_{Ar}−O−C oxygen atoms at the northern and southern termini of the $O(CH_2)_4O$ bridges form a rhombus rather than a square, visible in the second stereo-drawing for **16**⊙DMSO in Chart 2. The $C_{Ar}C_{Ar}C_{Ar}C_{Ar}$ planes (planes *a* of **28**) attached to the bridges are the reference points for the shift, distance, and diagonal parameters of Table 3, for comparison with the values in Table 2. The steric energies, the host−guest van der Waals energies, and the free surface areas of the host alone and in the presence of guest were calculated as before (see discussion of Table 2).

The values in Table 3 for the measured and calculated parameters for carceplex **16**⊙DMSO and its **18**⊙DMSO model provide interesting conclusions.

1. The crystal structure of **16**⊙DMSO in the molecule's complexing region is *near* a minimum-energy conformation. The distance and angle values of columns A (crystal structure) and B (MM3-minimized) are reasonably close to one another. The MM3-calculated steric energy of the crystal structure is 151 kcal mol^{-1} greater, and the free area of the host is 41 Å^2 less, than for the MM3-minimized model, chiefly due to the normalization by MM3 of bond distances to gas-phase minimum-energy values. The host−guest energy for the crystal structure is −18.6 compared to −18.8 kcal mol^{-1} for its model. The similarity of these values probably reflects a better model for the guest in **16**⊙DMSO compared to **15a**⊙DMF, as well as the loose fit of DMSO in the cavity of **16** (see below).

2. Host **16** of the crystal structure and of its MM3-idealized model changes very little upon inclusion of DMSO guest, as seen by a comparison of the values of columns A and B with those of C. The DMSO has no unusually short contacts with the host, in contrast to those of DMA inside **15**. In this connection it is noted that the decrease of free area for idealized host **18** when DMSO is included as guest is 5 Å^2 (column B, Table 3), much less than for idealized host **15b** with DMF (20 Å^2) or DMA (28 Å^2) as guest (columns B and D of Table 2). Furthermore, the cavity of host **16** is substantially larger (50% larger interhemispheric distance, Tables 2 and 3) and more spherical than that of **15** (CPK model and crystal structure parameter comparisons).

3. The DMSO guest reduces the steric energy of host **18** by about 17 kcal mol^{-1} (compare columns B and C of Table 3), somewhat more than the respective 11 and 5 kcal mol^{-1} by which DMF and DMA reduce the steric energy of host **15** (columns B, C, and D of Table 2). These three guest stabilizations of host correlate inversely with the relative steric constraints the host cavity places on the guest's freedom to locate itself in the cavity to increase the stability of the system. The constraints decrease in the order **15b**⊙DMA > **15b**⊙DMF > **18**⊙DMSO, which is in the reverse order of the values for the guest's release of the host's steric energy.

4. The crystal structure of **16**⊙DMSO shows the four $(CH_2)_4$ groups of the interbowl bridges to be located outside of the parallelepiped formed by the eight oxygen termini of these bridges (see last stereoview of Chart 2).

5. A more symmetrical conformation for the bowls is suggested by the approximate mirror planes in the crystal structure of **9**∪$(CH_3)_2CO$ (see Chart 2). A host molecule was modeled for **18**⊙DMSO in which the spanner conformations in the bowls were approximately related by two such perpendicular mirror planes. This model for **18**⊙DMSO comes closest among those calculated to what is obtained by constructing CPK models of **18**. Interestingly, the resulting parameter values,

Table 4. Chemical Shifts ($CDCl_3$ at 25 °C) Relative to $(CH_3)_4Si$ in ^1H NMR Spectra of DMA Free and Incarcerated, and Their Changes ($\Delta\delta$ Values) upon Incarceration in a Series of Hosts with Identical Hemispheres but Different Bridge Lengths

		bridges of hosts (structure numbers) whose spanners are OCH_2O and feet are CH_2CH_2Ph							
		OCH_2O (**15a**)[a]		$O(CH_2)_2O$ (**13**)[b]		$O(CH_2)_3O$ (**14**)[b]		$O(CH_2)_4O$ (**1**)[c]	
complexed guest protons	free guest δ	δ	$\Delta\delta$[d]	δ	$\Delta\delta$[d]	δ	$\Delta\delta$[d]	δ	$\Delta\delta$[d]
(a) H_3C, C=O, N, H_3C (c), CH_3 (b)	[a]H 2.08	−2.40	4.48	−1.98	4.06	−1.62	3.70	−1.64	3.72
	[b]H 3.02	−1.46	4.48	−0.99	4.01	−0.50	3.52	−0.42	3.44
	[c]H 2.94	1.04	1.90	1.39	1.55	1.43	1.51	1.61	1.33

[a] Taken from ref 7b. [b] This work. [c] Taken from ref 7c. [d] Defined as δ for free guest minus δ for incarcerated guest peaks.

listed in column D of Table 3, are not far from those for the MM3-minimized crystal structure of **18**⊙DMSO. Particularly noteworthy is the 152 kcal mol^{-1} value for the steric energy of this symmetrized structure, which is only 3 kcal mol^{-1} greater than the 149 kcal mol^{-1} value listed in column B for the less symmetrical model based on the crystal structure.

Imposing an approximate C_2 axis on each bowl (column E in Table 3) increases the steric energy of the carceplex by 10 kcal mol^{-1} over the observed conformation in column B. Small differences in the (strained) $C_{Ar}-O-C$ angles and size and shape of the cavity, as seen in the bridge lengths and free areas, accompany the energy change.

These results and the correlations implicit in the calculations suggest that **16**⊙DMSO in solution has a structure average not far from those modeled in columns B, D, and E of Table 3.

Correlations of ^1H NMR Spectral Properties with Structures of Carceplexes

Carceplexes **13**⊙DMA and **14**⊙DMA proved to be stable to temperatures in excess of 200 °C in $C_6D_5NO_2$. With a Bruker 500 MHz ^1H NMR instrument, the coalescence temperatures (T_c) and $\Delta G^{\ddagger}$ (kcal mol^{-1}) at T_c for rotations around the C−N bond of DMA in **13**⊙DMA and **14**⊙DMA were determined by the variable-temperature method as applied before to **15a**⊙DMA ($n = 1$, R = CH_2CH_2Ph) and to free DMA in $C_6D_5NO_2$.[7b] The T_c (°C) and $\Delta G^{\ddagger}$ (kcal mol^{-1}) values are respectively, for free DMA, 63 and 18.0; for **15a**⊙DMA, 190 and 20.3;[7b] for **13**⊙DMA, ≳167 and ≳20, for **14**⊙DMA, 134 and 18.2. Thus **14** containing four $O(CH_2)_3O$ bridging groups offers about the same constraints to rotation about the C−N bond of incarcerated DMA as does bulk solvent ($C_6D_5NO_2$), while **13** containing four $O(CH_2)_2O$ bridging groups offers about the same constraint as does **15** with four OCH_2O bridging groups. These results roughly correlate with conclusions drawn from CPK molecular model examinations, that **15**⊙DMA > **13**⊙DMA > **14**⊙DMA in internal strain.

Table 4 tabulates the chemical shifts (δ) in the ^1H NMR spectra of DMA dissolved in $CDCl_3$ at 25 °C, and of DMA incarcerated in the homologous series of dissolved hosts of identical structures (spanners are OCH_2O and feet are CH_2CH_2-Ph) whose four $O(CH_2)_nO$ bridges are $n = 1$ (**15a**),[7b] $n = 2$ (**13**), $n = 3$ (**14**), and $n = 4$ (**1**).[7c] The $\Delta\delta$ values for free and incarcerated DMA protons are also recorded in Table 4 and provide a measure of how tightly the three CH_3 groups of the guest are pressed into the polar caps, which are the hosts' most shielding region. The CH_3CO (a) protons in all cases are the most shielded, and incarceration provides upfield shift $\Delta\delta$ values of 4.48 ($n = 1$), 4.06 ($n = 2$), 3.70 ($n = 3$), and 3.72 ($n = 4$) ppm. The decreases in the values as the bridges increase in length and conformational flexibility are evident until $n = 3$ and $n = 4$, which provide essentially the same $\Delta\delta$ values. This leveling effect probably reflects a release of compression of the guest against the host which is introduced into the smaller hosts while the third and fourth bridges are formed, and which attenuates at the $n = 3$ and $n = 4$ bridge lengths.

Since the long polar axis of the host and the long axis of the guest must be aligned, the ^{b}H protons of the N−CH_3 *anti* to the C−CH_3 of DMA are the next most shielded of the incarcerated protons. They provide $\Delta\delta$ values of 4.48 ($n = 1$), 4.01 ($n = 2$), 3.52 ($n = 3$), and 3.44 ppm ($n = 4$), the first two of which are remarkably close to those of the *anti* ^{a}H protons located in the opposite hemisphere of the host. The ^{c}H protons of the N−CH_3 *syn* to the C−CH_3 of DMA are in the less shielded temperate zone of the globe. Accordingly their $\Delta\delta$ values are smaller, but exhibit a similar pattern as the host bridges become longer: $n = 1$, 1.90 ppm; $n = 2$, 1.55 ppm; $n = 3$, 1.51 ppm; $n = 4$, 1.33 ppm. Again the biggest decrease in shielding occurs in passing from the carceplex with the shortest to the carceplex with the next shortest bridge.

Summary

(1) In shell closures leading to 10 new host systems, some have been templated by guests whose incarcerations survive all four bridge formations and the isolation procedures. In other cases, the initial templating agent escapes incarceration either during formation of the final bridges or during isolation. Nonproductive self-complexation of cavitand starting materials in certain cases can inhibit shell closures. The lengths of the spanners have been varied to include $O(CH_2)_nO$ with $n = 1$, 2, or 3, and the bridges to include $O(CH_2)_nO$ with $n = 1-6$, and *m*-$OCH_2C_6H_4CH_2O$ groups. Three of the host systems have different spanners in their two hemispheres. (2) Crystal structures of **14**⊙NMP, **14**⊙DMA, and **16**⊙DMSO, in which the guests are located, are reported. Each host contains a center of symmetry. When the spanners are OCH_2O, the host contains a near C_4 axis, and the cavity is ellipsoidal, with the bridging carbons turned outward, and their terminal oxygen electron pairs turned inward. When the spanners are OCH_2CH_2O, the host contains a near C_2 axis, the cavity is more spherical, and the bridging carbons locate outward. The carbons of the spanners turn upward-inward, and their terminal oxygen electron pairs turn outward. Crystal structures of three cavitands with OCH_2O, $O(CH_2)_2O$, and $O(CH_2)_3O$ aryl-to-aryl spanners show that the bowls change their shapes substantially with changes in spanner length. The conformations of the OCH_2CH_2O spanners in cavitand **9** and hemicarcerand **16** are generally similar, but the hemispheric cavity of **16** is much closer to having a C_4 axis than that of **9**, and thus is complementary to more guest parts. (3) Energy-minimized structures for **15b**⊙DMF and **18**⊙DMSO are found to approach those of their related crystal structures. Free and guest-occupied areas of the host surfaces are compared, as well as steric energies and host−guest van der Waals energies. (4) Changes of $\Delta\delta$ values derived from ^1H NMR spectra of free and incarcerated guests are found to correlate well with expectations based on crystal structure determinations or CPK model examinations. Activation energies for rotations

about the C−N bond of DMA incarcerated in **15a**⊙DMA and **13**⊙DMA are higher than, and that for **14**⊙DMA is comparable to, that of free DMA in $C_6D_5NO_2$ as solvent. These relationships correlate well with expectations based on CPK model examinations of the complexes.

The complexation properties of new hosts **19**−**24** are under active investigation.

Experimental Section

General. All reactions were conducted under argon unless otherwise noted. Tetrahydrofuran (THF) was freshly distilled from benzophenone ketyl just prior to use. DMA,[8] NMP,[8] and DMSO[8] were degassed under high vacuum just before use. A Bruker ARX 500 MHz spectrometer was used to record ^{1}H NMR spectra unless otherwise noted. FAB MS were determined on a ZAB SE instrument with 3-nitrobenzyl alcohol (NOBA) as a matrix. Silica gel (E. Merck 63−200 μm) was used for flash chromatography, and gravity chromatography was performed on E. Merck silica gel (70−230 mesh). Thin-layer chromatography involved glass-backed plates (silica gel 60, F_{254}, 0.25 mm). Melting points (uncorrected) were measured on a Thomas-Hoover apparatus.

8,13,18,32-Tetrabromo-5,6,10,11,15,16,20,21-octahydro-1,25,27,29-tetrapentyl-2,24:3,23-dimetheno-1*H*,25*H*,27*H*,29*H*-bis[1,4]-dioxonino[6,5-*j*:6′,5′-*j*′]benzo[1,2-*e*:5,4-*e*′]bis[1,4]benzodioxonin Stereoisomer (8). To a stirred solution of 18 g (16.6 mmol) of **3** (R = $(CH_2)_4CH_3$)[5a] and 50 g (135 mmol) of $TsOCH_2CH_2OTs$ in 60 mL of DMSO was added 45 g (0.33 mol) of K_2CO_3. The mixture was stirred for 24 h at 25 °C and 4 days at 56 °C. The suspension was poured into 3 L of H_2O, filtered, and dried, and the residue was flash chromatographed on 600 g of silica gel with CH_2Cl_2−hexane (4:1 (v)) as the mobile phase to give 9.0 g (46%) of **8**: mp >300 °C; ^{1}H NMR ($CDCl_3$) δ 0.87 (t, J = 7.0 Hz, 12H, C*H*$_3$), 1.21−1.35 (m, 24H, (C*H*$_2$)$_3$), 2.05 (m, 8H, CHC*H*$_2$), 3.60−3.80 (m, 8H, inner OC*H*$_2$C*H*$_2$O), 4.26−4.48 (m, 8H, outer OC*H*$_2$C*H*$_2$O), 5.28 (t, J = 8.1 Hz, 4H, C*H* methine), 7.31 (s, 4H, Ar*H*); MS FAB *m/e* 1188 (M^+, 100). Anal. Calcd for $C_{56}H_{68}Br_4O_8$: C, 56.58; H, 5.77. Found: C, 56.51; H, 5.72.

8,13,18,32-Tetrahydroxy-5,6,10,11,15,16,20,21-octahydro-1,25,27,29-tetrapentyl-2,24:3,23-dimetheno-1*H*,25*H*,27*H*,29*H*-bis[1,4]-dioxonino[6,5-*j*:6′,5′-*j*′]benzo[1,2-*e*:5,4-*e*′]bis[1,4]benzodioxonin Stereoisomer (9). To a solution of 20.2 g (17 mmol) of **8** in 1 L of THF stirred at −78 °C was added 50 mL of a 2.2 M solution of *n*-BuLi−hexane (110 mmol) over 2 min. The solution was stirred for 10 min, and 50 mL of $B(OCH_3)_3$ (0.44 mol) was added over 2 min. The mixture was warmed to 25 °C and stirred for 1.5 h. The solution was cooled to −78 °C, and 500 mL of a 1.5 N NaOH solution in 15% aqueous H_2O_2 was added over 5 min. The solution was warmed to 25 °C, and careful addition of 100 g of $Na_2S_2O_5$ to the mixture followed by evaporation of THF under vacuum gave a solid, which was collected and air-dried. This material was dry-loaded onto a silica gel flash chromatography column (800 g in 3:1 (v) hexane−acetone). Elution of the column with 3:2 (v) hexane−acetone gave 9.7 g (61%) of **9**: mp 282−284 °C; ^{1}H NMR (CD_3COCD_3) δ 0.86 (t, J = 7.0 Hz, 12H, C*H*$_3$), 1.21−1.32 (m, 24H, (C*H*$_2$)$_3$), 2.15 (m, 8H, CHC*H*$_2$), 3.72 (m, 8H, inner OC*H*$_2$C*H*$_2$O), 4.27 (m, 8H, outer OC*H*$_2$C*H*$_2$O), 5.17 (t, J = 8.2 Hz, 4H, C*H* methine), 7.21 (s, 4H, Ar*H*), 7.61 (s, 4H, O*H*); MS FAB *m/e* 937 (M^+ + H, 100). Anal. Calcd for $C_{56}H_{72}O_{12}$: C, 71.79; H, 7.69. Found: C, 71.54; H, 7.54.

9,15,21,36-Tetrabromo-6,7,12,13,18,19,24,25-octahydro-1,29,31,33-tetrapentyl-2,28:3,27-dimetheno-1*H*,5*H*,11*H*,17*H*,23*H*,29*H*,31*H*,33*H*-bis[1,5]dioxecino[7,6-*k*:7′,6′-*k*′]benzo[1,2-*f*:5,4-*f*′]bis[1,5]-benzodioxecin Stereoisomer (10). A stirred mixture of 20 g (18.4 mmol) of **3** (R = $(CH_2)_4CH_3$), 50 g (0.13 mmol) of solvate-free $TsO(CH_2)_3OTs$, and 30 g (0.22 mol) of K_2CO_3 in 500 mL of DMSO was heated at 56 °C under argon for 4 days. The suspension was cooled to 25 °C, poured into 3 L of H_2O, and filtered, and the residue was flash chromatographed on 800 g of silica gel with CH_2Cl_2−hexane (4:1 (v)) as the mobile phase to give 9.2 g (40%) of **10**: mp >300 °C; ^{1}H NMR ($CDCl_3$) δ 0.86 (t, J = 7.1 Hz, 12H, C*H*$_3$), 1.19−1.32 (m, 24H, (C*H*$_2$)$_3$), 1.93−2.04 (m, 12H, CHC*H*$_2$, inner OCH$_2$C*H*$_2$CH$_2$O), 2.25−2.33 (m, 4H, outer OCH$_2$C*H*$_2$CH$_2$O), 3.97 (m, 8H, inner OC*H*$_2$-CH$_2$C*H*$_2$O), 4.65 (m, 8H, outer OC*H*$_2$CH$_2$C*H*$_2$O), 4.95 (t, J = 7.9 Hz, 4H, C*H* methine), 7.05 (s, 4H, Ar*H*); MS FAB *m/e* 1244 (M^+, 100). Anal. Calcd for $C_{60}H_{76}Br_4O_8$: C, 57.89; H, 6.15. Found: C, 58.18; H, 6.05.

9,15,21,36-Tetrahydroxy-6,7,12,13,18,19,24,25-octahydro-1,29,31,33-tetrapentyl-2,28:3,27-dimetheno-1*H*,5*H*,11*H*,17*H*,23*H*,29*H*,31*H*,33*H*-bis[1,5]dioxecino[7,6-*k*:7′,6′-*k*′]benzo[1,2-*f*:5,4-*f*′]bis[1,5]-benzodioxecin Stereoisomer (11). A stirred solution of 12 g (9.6 mmol) of tetrabromide **10** in 1 L of THF was cooled to −78 °C, and 50 mL of *n*-BuLi−hexane (120 mmol) was added over 2 min. After 10 min, 50 mL (524 mmol) of $B(OCH_3)_3$ was added and the mixture was warmed to 25 °C and stirred for 1.5 h. After treatment with 500 mL of a 1.5 N NaOH solution in 15% aqueous H_2O_2 and evaporation of the THF, the residue was flash chromatographed on silica gel (600 g). Elution with 3:1 (v) CH_2Cl_2−EtOAc gave 2.5 g (26%) of tetrol **11**: mp 260−262 °C; ^{1}H NMR ($CDCl_3$) δ 0.84 (t, J = 7.0 Hz, 12H, C*H*$_3$), 1.21−1.32 (m, 24H, (C*H*$_2$)$_3$), 1.82−2.05 (m, 16H, OCH$_2$C*H*$_2$-CH$_2$O, CHC*H*$_2$), 3.98 (m, 8H, inner OC*H*$_2$CH$_2$C*H*$_2$O), 4.53 (m, 8H, outer OC*H*$_2$CH$_2$C*H*$_2$O), 4.97 (t, J = 8.3 Hz, 4H, C*H* methine), 5.13 (s, 4H, O*H*), 6.97 (s, 4H, Ar*H*); MS FAB *m/e* 993 (M^+ + H, 100). Anal. Calcd for $C_{60}H_{80}O_{12}$: C, 72.55; H, 8.12. Found: C, 72.25; H, 8.13.

32,43-(Epoxyethanoxy)-18,22:53,57-dimethano-2,48:15,27-dimetheno-3,47,14,28-(methynoxyethanoxymethyno)-1*H*,16*H*,24*H*,26*H*,49*H*,51*H*-bis[1,3]benzodioxocino[9,8-*d*:9′,8′-*d*′]bis[1,3]benzodioxocino[9′,10′:15,16;10″,9‴:21,22][1,3,6,9,12,14,17,20]octaoxacyclodocosino[4,5-*j*:11,10-*j*′]bis[1,3]benzodioxocin, 8,9,37,38-Tetrahydro-1,16,24,26,49,51,59,72-octakis(2-phenylethyl)⊙*N*,*N*-Dimethylacetamide Stereoisomer (13⊙DMA).[9] Procedure A. Tetrol **7**[7a,12] (200 mg, 0.20 mmol), Cs_2CO_3 (1.9 g, 5.2 mmol), and $TsOCH_2CH_2OTs$ (160 mg, 0.43 mmol) were mixed in 200 mL of DMA. The stirred solution was warmed to 60 °C and stirred for 24 h. An additional 80 mg of the ditosylate was added and the solution stirred for 24 h at 80 °C. Again 80 mg of ditosylate was added and the solution stirred for 24 h at 100 °C. The solvent was evaporated under reduced pressure, and the residue was partitioned between 150 mL of H_2O and 200 mL of CH_2Cl_2. Brine (100 mL) was added, and the organic phase was separated through use of phase-separating filter paper. The organic layer was concentrated under vacuum to ≈5 mL, and the product was collected by filtration through a medium fritted glass funnel. The collected product was washed with CH_2Cl_2 (2 mL two times) and then with 3 mL of H_2O to give after drying at 80 °C at 10^{-5} Torr for 24 h 65 mg (29%) of **13**⊙DMA: mp >360 °C; ^{1}H NMR (200 MHz, $CDCl_3$) δ −1.98 (s, 3H, C*H*$_3$CO of DMA), −0.99 (s, 3H, NC*H*$_3$ of DMA), 1.39 (s, 3H, NC*H*$_3$ of DMA), 2.4−2.95 (m, 32H, C*H*$_2$C*H*$_2$Ph), 4.39 (d, J = 6.8 Hz, 8H, OC*H*$_2$O inner), 4.58 (s, 16H, OC*H*$_2$C*H*$_2$O), 4.85 (t, J = 7.7 Hz, 8H, C*H* methine), 5.85 (d, J = 6.8 Hz, 8H, OC*H*$_2$O outer), 6.80 (s, 8H, Ar*H*), 7.11−7.25 (m, 40H, C_6H_5); MS FAB *m/e* 2225 (M^+ + H, 90). Anal. Calcd for $C_{136}H_{120}O_{24} + C_4H_9NO$: C, 75.54; H, 5.84; N, 0.63; O, 17.96. Found: C, 75.54; H, 5.91; N, 0.58; O, 17.96.

33,45-(Epoxypropanoxy)-19,23:55,59-dimethano-2,50:16,28-dimetheno-3,49,15,29-(methynoxypropanoxymethyno)-1*H*,8*H*,17*H*,25*H*,27*H*,38*H*,51*H*,53*H*-bis[1,3]benzodioxocino[9,8-*d*:9′,8′-*d*′]bis[1,3]-benzodioxocino[9′,10′:16,17;10″,9‴:23,24][1,3,6,10,13,15,18,22] octaoxacyclotetracosino[4,5-*j*:12,11-*j*′]bis[1,3]benzodioxocin, 9,10,39,40-Tetrahydro-1,17,25,27,51,53,61,76-octakis(2-phenylethyl)⊙*N*,*N*-Dimethylacetamide Stereoisomer (14⊙DMA). Application of procedure A to 200 mg (0.20 mmol) of **7**, 1.7 g (5.2 mmol) of Cs_2CO_3, and 200 mg (0.52 mmol) of $TsO(CH_2)_3OTs$ (the additional aliquots were 100 mg each) gave 45 mg (20%) of **14**⊙DMA: mp >360 °C; ^{1}H NMR (200 MHz, $CDCl_3$) δ −1.62 (s, 3H, C*H*$_3$CO of DMA), −0.50 (s, 3H, NC*H*$_3$ of DMA), 1.43 (s, 3H, NC*H*$_3$ of DMA), 2.19 (t, J = 6.0 Hz, 8H, OCH$_2$C*H*$_2$CH$_2$O), 2.44−2.68 (m, 32H, C*H*$_2$C*H*$_2$Ph), 4.19 (t, J = 6.0 Hz, 16H, OC*H*$_2$CH$_2$C*H*$_2$O), 4.34 (d, J = 6.9 Hz, 8H, OC*H*$_2$O inner), 4.84 (t, J = 7.7 Hz, 8H, C*H* methine), 5.81 (d, J = 6.9 Hz, 8H, OC*H*$_2$O outer), 6.83 (s, 8H, Ar*H*), 7.08−7.24 (m, 40H, C_6H_5); MS FAB *m/e* 2281 (M^+ + H, 95). Anal. Calcd for $C_{140}H_{128}O_{24} + C_4H_9NO$: C, 75.79; H, 6.08; N, 0.61; O, 17.54. Found: C, 75.47; H, 6.04; N, 0.54; O, 17.88.

Procedure A was also applied to the preparation of **14**⊙NMP (15%): ^{1}H NMR (360 MHz, $CDCl_3$) δ −1.07 (m, 2H, NCH$_2$C*H*$_2$CH$_2$ of NMP), −0.84 (s, 3H, NC*H*$_3$ of NMP), −0.73 (t, J = 7.5 Hz, 2H, NC*H*$_2$ of NMP), 1.94 (m, 2H, NCOC*H*$_2$ of NMP), 2.20 (m, 8H, OCH$_2$C*H*$_2$CH$_2$O), 2.48 (m, 16H, C*H*$_2$CH$_2$Ph), 2.66 (m, 16H, CH$_2$C*H*$_2$-Ph), 4.15 (m, 16H, OC*H*$_2$CH$_2$C*H*$_2$O), 4.33 (d, J = 7.1 Hz, 8H, OC*H*$_2$O inner), 4.83 (t, J = 7.9 Hz, 8H, C*H* methine), 5.82 (d, J = 7.1 Hz, 8H, OC*H*$_2$O outer), 6.85 (s, 8H, Ar*H*), 7.16−7.23 (m, 40H, C_6H_5); MS FAB

m/e 2294.6 ($M^+ + H$, 100). Anal. Calcd for $C_{140}H_{128}O_{24} + C_5H_9NO$: C, 75.93; H, 6.02. Found: C, 76.29; H, 5.98.

2,3,5,6,9,10,11,12,15,16,19,20,24,25,35,36,40,41,44,45,46,47,50,51,55,56,66,67-Octacosahydro-1,20,29,31,60,62,71,88-octapentyl-38,53-(epoxybutanoxy)-22,27:64,69-dimethano-2,59:19,32-dimetheno-3,58,18,33-(methynoxybutanoxymethyno)-1*H*,18*H*,29*H*,31*H*,60*H*,62*H*-bis[1,4]benzodioxonino[10,9-*e*:10′,9′-*e*′]bis[1,4]benzodioxonino[10′,11′:8,9;11″,10‴:16,17][1,4,7,10,15,18,21,24]octaoxacyclooctacosino[3,2-*k*:22,23-*k*′]bis[1,4]benzodioxonin⊙Dimethyl Sulfoxide Stereoisomer (16⊙DMSO). Procedure B. A solution of 455 mg (0.49 mmol) of dry tetrol 9 and 600 mg (1.5 mmol) of $TsO(CH_2)_4OTs$[8] in 80 mL of DMSO was added via a syringe pump over 20 h to a stirred suspension of 6 g (18.4 mmol) of Cs_2CO_3 in 350 mL of DMSO at 74 °C under argon. An additional 400 mg (1 mmol) of the ditosylate was added, and the mixture was heated at 74 °C for an additional 24 h. The solvent was evaporated under vacuum, and the residue was partitioned between $CHCl_3$ and 10% aqueous NaCl. The organic layer was dried and filtered, the solvent was evaporated under vacuum to about 10 mL, and this material was flash chromatographed on 100 g of silica gel in CH_2Cl_2. Elution of the column with 24:1 (v) CH_2Cl_2−Et_2O gave 45 mg (9%) of 16⊙DMSO: mp >300 °C; ^{1}H NMR ($CDCl_3$) δ −0.80 (s, 6H, S*CH*$_3$ of DMSO), 0.85 (t, J = 7.1 Hz, 24H, C*H*$_3$CH$_2$), 1.20−2.11 (m, 80H, C*H*$_2$), 3.48 (m, 16H, inner OC*H*$_2$C*H*$_2$O), 4.15 (m, 32H, bridge OC*H*$_2$, outer OC*H*$_2$C*H*$_2$O), 5.00 (t, J = 8.0 Hz, 8H, C*H* methine), 6.96 (s, 8H, Ar*H*); MS FAB *m/e* 2167 (M^+, 100). Anal. Calcd for $C_{128}H_{168}O_{24} + C_2H_6OS$: C, 71.99; H, 8.09. Found: C, 71.85; H, 8.13.

2,3,5,6,10,11,12,13,16,17,20,21,25,26,36,37,41,42,46,47,48,49,52,53,57,58,68,69-Octacosahydro-1,21,30,32,62,64,73,92-octapentyl-39,55-(epoxypentanoxy)-23,28:66,71-dimethano-2,61:20,33-dimetheno-3,60,19,34-(methynoxypentanoxymethyno)-1*H*,9*H*,19*H*,30*H*,32*H*,45*H*,62*H*,64*H*-bis[1,4]benzodioxonino[10,9-*e*:10′,9′-*e*′]bis[1,4]benzodioxonino[10′,11′:8,9;11″,10‴:17,18][1,4,7,10,16,19,22,25]octaoxacyclotriacontino[3,2-*k*:23,24-*k*′]bis[1,4]benzodioxonin Stereoisomer (17). Application of procedure B to 450 mg (0.48 mmol) of tetrol 9 and 0.60 g (1.4 mmol) of $TsO(CH_2)_5OTs$[8] in 80 mL of DMA (initial addition, and 0.40 g final addition, second heating, 24 h) gave 77 mg (7.5%) of 17: mp >300 °C; ^{1}H NMR ($CDCl_3$) δ 0.86 (t, J = 7.1 Hz, 24H, C*H*$_3$CH$_2$), 1.23−2.09 (m, 88H, C*H*$_2$), 3.53 (m, 16H, inner OC*H*$_2$C*H*$_2$O), 3.75−4.12 (m, 32H, bridge OC*H*$_2$, outer OC*H*$_2$C*H*$_2$O), 5.11 (t, J = 8.0 Hz, 8H, C*H* methine), 6.96 (s, 8H, Ar*H*); MS FAB *m/e* 2145 (M^+, 100). Anal. Calcd for $C_{132}H_{176}O_{24}\cdot 3H_2O$: C, 72.04; H, 8.34. Found: C, 71.87; H, 7.94.

Procedure C for Conversion of Tetrols 6, 9, and 11 into Their Tetraethers 25, 26, and 27, Respectively. These tetrols were treated with a very large excess of 1,3-$(ClCH_2)_2C_6H_4$ and Cs_2CO_3 in NMP[8] at 25 °C stirred under argon. After completion of the reaction, the suspension was poured into 800 mL of 5% aqueous NaCl, filtered, and dried and the residue was flash chromatographed on 100 g of silica gel. Elution of the column with 3:2 and 4:1 (v) CH_2Cl_2−hexane mixtures gave the desired tetrachloride.

1,21,23,25-Tetrapentyl-2,20:3,19-dimetheno-1*H*,21*H*,23*H*,25*H*-bis[1,3]dioxocino[5,4-*i*:5′,4′-*i*′]benzo[1,2-*d*:5,4-*d*′]bis[1,3]benzodioxocin, 7,11,15,28-Tetrakis((3-(chloromethyl)phenyl)methoxy), Stereoisomer (25). A mixture of 0.6 g (0.68 mmol) of **6**,[6] 6 g (34.2 mmol) of 1,3-$(ClCH_2)_2C_6H_4$, and 6 g (18.4 mmol) of Cs_2CO_3 in 200 mL of NMP at 25 °C was stirred for 17 h. Application of procedure C gave 587 mg (60%) of **25**, mp >300 °C: ^{1}H NMR ($CDCl_3$) δ 0.92 (t, J = 7.0 Hz, 12H, C*H*$_3$CH$_2$), 1.25−1.48 (m, 24H, (C*H*$_2$)$_3$), 2.21 (m, 8H, CHC*H*$_2$), 4.44 (d, J = 7.1 Hz, 4H, inner OC*H*$_2$O), 4.59 (s, 8H, ArC*H*$_2$), 4.75 (t, J = 8.1 Hz, 4H, C*H* methine), 4.95 (s, 8H, ArOC*H*$_2$), 5.78 (d, J = 7.1 Hz, 4H, outer OC*H*$_2$O), 6.84 (s, 4H, Ar*H*), 7.30−7.51 (m, 16H, Ar*H*); MS FAB *m/e* 1434 (M^+, 100). Anal. Calcd for $C_{84}H_{92}Cl_4O_{12}$: C, 70.29; H, 6.46. Found: C, 70.06; H, 6.55.

8,13,18,32-Tetrakis((3-(chloromethyl)phenyl)methoxy)-1,25,27,29-tetrapentyl-5,6,10,11,15,16,20,21-octahydro-2,24:3,23-dimetheno-1*H*,25*H*,27*H*,29*H*-bis[1,4]dioxocino[6,5-*j*:6′,5′-*j*′]benzo[1,2-*e*:5,4-*e*′]bis[1,4]benzodioxonin Stereoisomer (26). A mixture of 0.6 g (0.64 mmol) of **9**, 3.2 g (18.3 mmol) of 1,3-$(ClCH_2)_2C_6H_4$, and 6 g (18.4 mmol) of Cs_2CO_3 in 200 mL of NMP was stirred at 25 °C under argon for 2 days. Application of procedure C gave 660 mg (69%) of **26**: mp 295 °C dec; ^{1}H NMR ($CDCl_3$) δ 0.89 (t, J = 7.0 Hz, 12H, C*H*$_3$-CH$_2$), 1.24−1.39 (m, 24H, (C*H*$_2$)$_3$), 2.06−2.12 (m, 8H, CHC*H*$_2$), 3.70 (m, 8H, inner OC*H*$_2$C*H*$_2$O), 4.29 (m, 8H, outer OC*H*$_2$C*H*$_2$O), 4.60 (s, 8H, ArC*H*$_2$), 5.07 (s, 8H, ArOC*H*$_2$), 5.17 (t, J = 8.1 Hz, 4H, C*H* methine), 7.02 (s, 4H, Ar*H*), 7.31−7.44 (m, 12H, Ar*H*), 7.57 (s, 4H, Ar*H*); MS FAB *m/e* 1491 (M^+, 100). Anal. Calcd for $C_{88}H_{100}Cl_4O_{12}$: C, 70.86; H, 6.76. Found: C, 70.78; H, 6.73.

9,15,21,36-Tetrakis((3-(chloromethyl)phenyl)methoxy)-6,7,12,13,18,19,24,25-octahydro-1,29,31,33-tetrapentyl-2,28:3,27-dimetheno-1*H*,5*H*,11*H*,17*H*,23*H*,29*H*,31*H*,33*H*-bis[1,5]dioxocino[7,6-*k*:7′,6′-*k*′]benzo[1,2-*f*:5,4-*f*′]bis[1,5]benzodioxocin Stereoisomer (27). A mixture of 940 mg (0.95 mmol) of tetrol **11**, 8 g (45.7 mmol) of 1,3-$(ClCH_2)_2C_6H_4$, and 6 g (18.4 mmol) of Cs_2CO_3 in 200 mL of NMP was stirred for 2 days under argon at 25 °C. Application of procedure C gave 0.92 g (63%) of **27**: mp >300 °C; ^{1}H NMR ($CDCl_3$) δ 0.88 (t, J = 6.9 Hz, 12H, C*H*$_3$CH$_2$), 1.14−1.91 (m, 32H, (C*H*$_2$)$_3$, OCH$_2$C*H*$_2$-CH$_2$O), 2.07 (m, 8H, CHC*H*$_2$), 3.92−4.03 (m, 8H, inner OC*H*$_2$-CH$_2$C*H*$_2$O), 4.64 (m, 16H, outer OC*H*$_2$CH$_2$C*H*$_2$O, ArC*H*$_2$), 4.96 (s, 8H, ArOC*H*$_2$), 5.13 (t, J = 8.2 Hz, 4H, C*H* methine), 7.30−7.43 (m, 16H, Ar*H*), 7.53 (s, 4H, Ar*H*); MS FAB *m/e* 1547 (M^+, 100). Anal. Calcd for $C_{92}H_{108}Cl_4O_{12}$: C, 71.40; H, 7.03. Found: C, 71.22; H, 6.99.

General Procedure D. This procedure was applied to the isolation of hemicarcerands **19**−**24** from their reaction mixtures. The solvent was evaporated under vacuum, the residue was partitioned between $CHCl_3$ and 10% aqueous NaCl, and the $CHCl_3$ layer was dried ($MgSO_4$), concentrated, and flash chromatographed on silica gel (125 g). Elution of the column with 4:1 (v) CH_2Cl_2−hexane and CH_2Cl_2 gave the hemicarcerand.

14*H*,48*H*-37,53-(Epoxymethano[1,3]benzenomethanoxy)-23,27:63,67-dimethano-2,58:9,13:20,32:43,47-tetrametheno-3,57,19,33-(methynoxymethano[1,3]benzenomethanoxymethyno)-1*H*,8*H*,21*H*,29*H*,31*H*,42*H*,59*H*,61*H*-bis[1,3]benzodioxocino[9,8-*d*:9′,8′-*d*′]bis[1,3]benzodioxocino[9′,10′:20,21;10″,9‴:31,32][1,3,6,14,17,19,22,30]octaoxacyclodotriacontino[4,5-*j*:16,15-*j*′]bis[1,3]benzodioxocin, 1,21,29,31,59,61,69,95-Octapentyl-, Stereoisomer (19). A mixture of 0.5 g (0.57 mmol) of **6**,[6] 0.50 g (2.86 mmol) of 1,3-$(ClCH_2)_2C_6H_4$, and 4 g (12.3 mmol) of Cs_2CO_3 in 425 mL of NMP was stirred at 25 °C for 66 h under argon. A 0.5 g (2.86 mmol) additional portion of 1,3-$(ClCH_2)_2C_6H_4$ was added, the temperature was raised to 60 °C, and stirring was continued for 2 days. Application of procedure D to the reaction mixture gave 308 mg (50%) of **19**: mp >300 °C; ^{1}H NMR ($CDCl_3$) δ 0.94 (t, J = 7.1 Hz, 24H, C*H*$_3$CH$_2$), 1.3−1.5 (m, 48H, (C*H*$_2$)$_3$), 2.15 (m, 16H, CHC*H*$_2$), 4.19 (d, J = 7.1 Hz, 8H, inner OC*H*$_2$O), 4.72 (t, J = 8.1 Hz, 8H, C*H* methine), 4.83 (s, 16H, ArC*H*$_2$), 5.45 (d, J = 7.1 Hz, 8H, outer OC*H*$_2$O), 6.82 (s, 8H, Ar*H*), 7.18−7.34 (m, 12H, Ar*H*), 7.46 (s, 4H, Ar*H*); MS FAB *m/e* 2169.5 (M^+, 100). Anal. Calcd for $C_{136}H_{152}O_{24}$: C, 75.28; H, 7.01. Found: C, 74.99; H, 6.96.

The same hemicarcerand (**19**) with identical physical properties was prepared in 2.2% yield from tetrachloride **25** and tetrol **6**[6] by a procedure similar to the preparation of **20** from tetrachloride **26** and tetrol **9** (see below).

2,3,5,6,18,19,22,23,27,28,38,39,43,44,56,57,61,62,72,73-Eicosahydro-1,23,32,34,66,68,77,103-octapentyl-15*H*,53*H*-41,59-(epoxymethano[1,3]benzenomethanoxy)-25,30:70,75-dimethano-2,65:10,14:22,35:48,52-tetrametheno-3,64,21,36-(methynoxymethano[1,3]benzenomethanoxymethyno)-1*H*,9*H*,21*H*,32*H*,34*H*,47*H*,66*H*,68*H*-bis[1,4]dioxonino[10,9-*e*:10′,9′-*e*′]bis[1,4]benzodioxonino[10′,11′:8,9;11″,10‴:19,20][1,4,7,10,18,21,24,27]octaoxacyclotetratriacontino[3,2-*k*:25,26-*k*′]bis[1,4]benzodioxonin Stereoisomer (20). A mixture of 360 mg (0.38 mmol) of tetrol **9**, 580 mg (0.39 mmol) of tetrachloride **26**, 6 g of Cs_2CO_3 (18.4 mmol), and 400 mL of NMP was stirred for 20 h at 25 °C under argon and then heated at 60 °C for 40 h. Application of procedure D to the reaction mixture gave 376 mg (43%) of **20**: mp >300 °C; ^{1}H NMR ($CDCl_3$) δ 0.89 (t, J = 7.0 Hz, 24H, C*H*$_3$CH$_2$), 1.26−1.45 (m, 48H, (C*H*$_2$)$_3$), 2.10−2.14 (m, 16H, CHC*H*$_2$), 3.47−3.56 (m, 16H, inner OC*H*$_2$C*H*$_2$O), 3.92−4.06 (m, 16H, outer OC*H*$_2$C*H*$_2$O), 5.10−5.19 (m, 24H, ArC*H*$_2$, C*H* methine), 7.05−7.33 (m, 20H, Ar*H*), 7.88 (s, 4H, Ar*H*); MS FAB *m/e* 2282.8 ($M^+ + H$, 100). Anal. Calcd for $C_{144}H_{168}O_{24}$: C, 75.76; H, 7.42. Found: C, 75.36; H, 7.26.

In an alternative approach to the synthesis of **20** using tetrol **9** and 1,3-$(ClCH_2)_2C_6H_4$ by the method applied for the synthesis of **19**, an 8% yield of **20** was obtained, which was identified by its ^{1}H NMR.

2,3,6,7,20,21,24,25,30,31,42,43,48,49,62,63,68,69,80,81-Eicosahydro-1,25,35,37,73,75,85,111-octapentyl-16*H*,58*H*-45,65-(epoxymethano[1,3]benzenomethanoxy)-27,33:77,83-dimethano-2,72:11,15:24,38:53,57-tetrametheno-3,71,23,39-(methynoxymethano[1,3]benzenomethanoxymethyno)-1*H*,5*H*,10*H*,19*H*,23*H*,29*H*,35*H*,37*H*,41*H*,47*H*,52*H*,61*H*,67*H*,73*H*,75*H*,79*H*-bis[1,5]benzodioxecino[11,10-*f*:11′,10′-*f*′]bis[1,5]benzodioxecino[11′,12′:9,10; 12″,11″:20,21][[1,4,8,11,19,22,26,29]octaoxacyclohexatriacontino[3,2-*l*:27,28-*l*′]bis[1,5]benzodioxecin Stereoisomer (21). A mixture of 154 mg (0.15 mmol) of tetrol **11**, 240 mg (0.15 mmol) of tetrachloride **27**, 8 g (47.6 mmol) of 1,2,3-$(CH_3O)_3C_6H_3$, 5 g (15.3 mmol) of Cs_2CO_3, and 160 mL of NMP was stirred for 24 h at 25 °C under argon and then heated 48 h at 60 °C. Application of procedure D to the reaction mixture gave 22 mg (6%) of **21**: mp >300 °C; ^{1}H NMR ($CDCl_3$) δ 0.85 (t, J = 7.0 Hz, 24 H, CH_3CH$_2$), 1.24−1.34 (m, 48H, (CH_2)$_3$), 1.84 (m, 8H, inner OCH$_2$CH_2CH$_2$O), 2.21 (m, 24H, CHCH_2, outer OCH$_2$CH_2CH$_2$O), 3.86 (m, 16H, inner OCH_2CH$_2$CH_2O), 4.38 (m, 16H, outer OCH_2-CH$_2$CH_2O), 5.06 (t, J = 8.3 Hz, 8H, CH methine), 5.19 (s, 16H, ArCH_2), 7.04−7.30 (m, 20H, ArH), 8.02 (s, 4H, ArH); MS FAB *m/e* 2394.9, (M^+ + H, 100). Anal. Calcd for $C_{152}H_{184}O_{24}\cdot 6H_2O$: C, 72.93; H, 7.89. Found: C, 72.87; H, 8.87.

In an alternative approach to the synthesis of **21** using tetrol **11** and 1,3-$(ClCH_2)_2C_6H_4$, no detectable amount of **21** was obtained.

2,3,17,18,21,22,26,27,37,38,42,43-Dodecahydro-1,22,31,33,63,65,73,99-octapentyl-14*H*,52*H*-40,57-(epoxymethano[1,3]benzenomethanoxy)-24,29:67,71-dimethano-2,62:9,13:21,34:47,51-tetrametheno-3,61,20,35-(methynoxymethano[1,3]benzenomethanoxymethyno)-1*H*,8*H*,20*H*,31*H*,33*H*,46*H*,63*H*,65*H*-[1,3]-benzodioxocino[9,10-*d*][1,3]benzodioxocino[9‴,8‴:4′,5′][1,3]benzodioxocino[10′,9′-*f*$_1$][1,4]benzodioxonino[11″,10″-*o*][1,4]benzodioxonino[10⁗,9⁗:5‴,6‴] [1,4]benzodioxonino[10‴,11‴-*u*]-[1,3,6,14,17,20,23,31]octaoxacyclotritriacontin Stereoisomer (22). A mixture of 320 mg (0.34 mmol) of tetrol **9**, 520 mg (0.36 mmol) of tetrachloride **25**, 5 g of Cs_2CO_3 (15.3 mmol), and 400 mL of NMP was stirred for 20 h at 25 °C under argon and 62 h at 62 °C. Application of procedure D to the reaction mixture provided 160 mg (21%) of **22**: mp >300 °C; ^{1}H NMR ($CDCl_3$) δ 0.88−0.96 (m, 24H, CH_3CH$_2$), 1.23−1.53 (m, 48H, (CH_2)$_3$), 2.06−2.22 (m, 16H, CHCH_2), 3.50−4.24 (m, 20H, OCH_2CH$_2$O, inner OCH_2O), 4.71 (t, J = 8.1 Hz, 4H, CH methine), 4.87 (s, 8H, ArCH_2), 5.11 (t, J = 8.2 Hz, 4H, CH methine), 5.16 (s, 8H, ArCH_2), 5.53 (d, J = 7.1 Hz, 4H, outer OCH_2O), 6.85 (s, 4H, ArH), 7.04−7.62 (m, 20H, ArH); MS FAB *m/e* 2226.3 (M^+ + H, 100). Anal. Calcd for $C_{140}H_{160}O_{24}$: C, 75.51; H, 7.24. Found: C, 75.24; H, 7.02.

In an alternative approach to the synthesis of **22**, a mixture of 300 mg (0.34 mmol) of tetrol **6**,[6] 508 mg (0.34 mmol) of tetrachloride **26**, 5 g (15.3 mmol) of Cs_2CO_3, and 400 mL of NMP under argon was stirred at 25 °C (20 h) and then heated at 62 °C (48 h). Application of procedure D to the reaction mixture gave 15 mg (2%) of **22**, identified by its ^{1}H NMR.

3,4,7,8,13,14,25,26,31,32,51,52-Dodecahydro-8,18,20,52,54,62,91,104-octapentyl-41*H*,75*H*-28,46-(epoxymethano[1,3]benzenomethanoxy)-10,16:56,60-dimethano-7,21:36,40:51,63:70,74-tetrametheno-6,22,50,64-(methynoxymethano[1,3]benzenomethanoxymethyno)-2*H*,6*H*,12*H*,18*H*,20*H*,24*H*,30*H*,35*H*,50*H*,54*H*,62*H*,69*H*-[1,5]benzodioxecino[12,11-*o*][1,5]benzodioxecino[11⁗,10⁗:6′,7′][1,5]benzodioxecino[11′,12′-*v*][1,3]-benzodioxocino[9″,10″-*d*][1,3]benzodioxocino[9⁗,8⁗:4‴,5‴] [1,3]-benzodioxocino[10‴,9‴-*g*$_1$][1,3,6,14,17,21,24,32]-octaoxacyclotetratriacontin Stereoisomer (23). A mixture of 335 mg (0.34 mmol) of tetrol **11**, 490 mg (0.34 mmol) of tetrachloride **25**, 20 g (119 mmol) of 1,2,3-$(CH_3O)_3C_6H_3$, 5 g (15.3 mmol) of Cs_2CO_3, and 400 mL of NMP was stirred for 18 h at 25 °C under argon and then heated for 48 h at 60 °C. Application of prodecure D to the reaction mixture gave 15 mg (1.8%) of **23**⊙1,2,3-$(CH_3O)_3C_6H_3$: mp >300 °C; ^{1}H NMR ($CDCl_3$) δ −0.12 (s, 6H, OCH_3), 0.90−0.97 (m, 24H, CH_3CH$_2$), 1.25−1.45 (m, 48H, (CH_2)$_3$), 2.05−2.27 (m, 24H, CHCH_2, OCH$_2$CH_2CH$_2$O), 3.01 (s, 3H, OCH_3), 4.01 (m, 8H, inner OCH_2CH$_2$CH_2O), 4.26−4.37 (m, 12H , inner OCH_2O, outer OCH_2-CH$_2$CH_2O), 4.80−4.98 (m, 24H, ArCH_2, CH methine), 5.22 (d, J = 8.2 Hz, 2H, ArH), 5.58 (d, J = 7.1 Hz, 4H, outer OCH_2O), 6.45 (m, 1H, ArH), 6.90−7.35 (m, 24H, ArH); MS FAB *m/e* 2449.4 (complex, 100), *m/e* 2281.4 (free **23**, 80). Anal. Calcd for $C_{144}H_{168}O_{24}\cdot C_9H_{12}O_3$: C, 74.97; H, 7.40. Found: C, 75.66; H, 7.88.

A similar experiment with tetrol **11** and tetrachloride **25** in the absence of 1,2,3-$(CH_3O)_3C_6H_3$ gave no detectable amount of **23**. The reaction of tetrol **6** and tetrachloride **27** also failed to give **23** under similar conditions with or without 1,2,3-$(CH_3O)_3C_6H_3$.

2,3,5,6,19,20,23,24,29,30,41,42,47,48,60,61,65,66,76,77-Eicosahydro-1,24,34,36,70,72,81,106-octapentyl-15*H*,57*H*-44,63-(epoxymethano[1,3]benzenomethanoxy)-26,32:74,79-dimethano-2,69:10,14:23,37:52,56-tetrametheno-3,68,22,38-(methynoxymethano[1,3]-benzenomethanoxymethyno)-1*H*,9*H*,18*H*,22*H*,28*H*,34*H*,36*H*,40*H*,46*H*,51*H*,70*H*,72*H*-[1,5]benzodioxecino[12,11-*s*][1,5]benzodioxecino[11⁗,10⁗:6′,7′][1,5]benzodioxecino[11′,12′-*z*][1,4]benzodioxonino[10″,11″-*h*][1,4]benzodioxonino[10⁗,9⁗: 5‴,6‴][1,4]-benzodioxonino[11‴,10‴-*b*][1,4,7,10,18,21,25,28]-octaoxacyclopentatriacontin Stereoisomer (24). A mixture of 342 mg (0.34 mmol) of tetrol **11**, 510 mg (0.34 mmol) of tetrachloride **26**, and 6 g (18.4 mmol) of Cs_2CO_3 in 425 mL of NMP under argon was heated for 18 h at 70 °C. Application of prodecure D to the reaction mixture gave 242 mg (30%) of **24**: mp >300 °C; ^{1}H NMR ($CDCl_3$) δ 0.87 (m, 24H, CH_3CH$_2$), 1.12−1.37 (m, 48H, (CH_2)$_3$), 1.98−2.13 (m, 24H, CHCH_2, OCH$_2$CH_2CH$_2$O), 3.62−3.75 (m, 16H, inner OCH_2CH_2O, inner OCH_2CH$_2$CH_2O), 4.01 (m, 8H , outer OCH_2CH_2O), 4.58 (m, 8H, outer OCH_2CH$_2$CH_2O), 5.06−5.15 (m, 24H, ArCH_2, CH methine), 7.03−7.32 (m, 20H, ArH), 7.95 (s, 4H, ArH); MS FAB *m/e* 2338.2 (M^+ + H, 100). Anal. Calcd for $C_{148}H_{176}O_{24}$: C, 76.00; H, 7.58. Found: C, 75.89; H, 7.55.

In an alternative synthesis of **24**, a mixture of 115 mg (0.12 mmol) of tetrol **9**, 190 mg (0.12 mmol) of **27**, and 4.0 g of Cs_2CO_3 in 180 mL of NMP under argon was heated at 70 °C for 38 h. Application of procedure D gave 57 mg (20%) of **24**. The 500 MHz ^{1}H NMR spectrum of this sample was identical to that of the material prepared from **11** and **26**.

Crystal Structures

General. With the exception of **12**, all data were collected with Cu $K\alpha$ radiation at 25 °C, and all structures were solved by direct methods (SHELX86 or SHELXS90).[16a] For **12**, data were collected at 128 K with Mo $K\alpha$ radiation and the structure was solved by heavy atom methods. All refinements were carried out with SHELX76,[16b] all phenyl rings were treated as rigid groups, and hydrogen atoms, when included, were placed in calculated positions (C−H = 1.08 Å).

Tetrol **9** was crystallized from acetone to give **9**∪$(CH_3)_2$-CO·$(CH_3)_2$CO·2H$_2$O, space group $P2_1/n$, a = 16.24(1) Å, b = 22.81(2) Å, c = 17.58(1) Å, β = 101.36(2)°, V = 6383 Å^3, Z = 4, 8755 unique reflections, 4219 with $I > 2\sigma(I)$, $2\theta_{max}$ = 115°, R = 0.11. Only oxygen and host methyl and methylene carbon atoms were refined anisotropically. One molecule of acetone is located in the host cavity (see Chart 2). The guest acetone is partially disordered, as is one pentyl 'foot'. Solvent water is probably disordered also. Closest O···O approaches between molecules are between a hydroxyl oxygen and the nonguest acetone, 2.67(2) Å, between another hydroxyl oxygen and the water molecules, 3.08(2) and 3.13(2) Å, and between a third and fourth hydroxyl oxygen and bridging oxygen atoms from two different symmetry-related host molecules, 2.81 and 2.92(2) Å, suggesting an extensive system of hydrogen bonding.

Tetrabromocavitand **12** was crystallized from $CHCl_2CHCl_2$, space group Cm, a = 8.887(1) Å, b = 24.148(3) Å, c = 9.173(1) Å, β = 100.585(4)°, V = 1935 Å^3, Z = 2, 1762 unique reflections, 1646 with $I > 3\sigma(I)$, $2\theta_{max}$ = 50°, R = 0.034. Only bromine atoms were refined anisotropically. No solvent molecules were found in the crystal. A mirror plane through the two "up" rings bisects the molecule (see Chart 2).

Carceplex **14**⊙NMP∪2$C_6H_5NO_2$·2$C_6H_5NO_2$ was crystallized from $CHCl_3$−$C_6H_5NO_2$, space group $P\bar{1}$, a = 12.216(3) Å, b

(16) (a) Sheldrick, G. M. *Acta Crystallogr.* **1990**, *A46*, 467−473. (b) Sheldrick, G. M. *SHELX76*; University of Cambridge, U.K., 1976.

= 26.288(7) Å, c = 11.740(6) Å, α = 101.93(3)°, β = 107.36(3)°, γ = 88.51°, V = 3518 Å^3, Z = 1, 8046 unique reflections, 2180 with $I > 2\sigma(I)$, $2\theta_{max} = 105°$, $R = 0.134$. No atoms were refined with anisotropy. Refinement was carried out in two blocks, 234 hemicarcerand parameters and 78 solvent and guest parameters. The host is centrosymmetric, and *N*-methylpyrrolidinone (NMP) is disordered between two positions related by the center of symmetry in the host cavity. No hydrogen atoms have been included for the guest molecule. Two $C_6H_5NO_2$ molecules are each surrounded by one set of four CH_2-CH_2Ph "feet" attached to one hemisphere of the host. Two other solvent $C_6H_5NO_2$ molecules (per host molecule) are located between the hemicarceplexes. The two cavitand moieties are slipped (2.36 Å) with respect to each other (see Chart 2). The least-squares plane through the seven atoms of the guest conforms to the shape of the cavity as described by the box with the eight bridge O atoms at the corners and is nearly equidistant from each bridge O atom of the pairs related by the center of symmetry. The planes through the four bridge oxygen atoms of each cavitand moiety (planar within 0.02 Å) are 3.4 Å apart, and the angles between the normals to these planes and the guest plane are 60°.

The crystal structure of **14**⊙DMA∪2$CHCl_3$·6$CHCl_3$, crystallized from $CHCl_3$−$C_6H_5NO_2$−C_2H_5OH, space group $P\bar{1}$, a = 16.457(7) Å, b = 19.459(2) Å, c = 12.457(4) Å, α = 93.712-(16)°, β = 96.47(3)°, γ = 102.008(17)°, V = 3851 Å^3, Z = 1, 8019 unique reflections, 4706 with $I > 2\sigma(I)$, $2\theta_{max} = 100°$, was refined to $R = 0.17$. Chlorine atoms were refined with anisotropy. The host is centrosymmetric, and the DMA guest is disordered over two overlapping sites in the host cavity (related by the center of symmetry). No H atoms have been included for the guest molecule, and all other guest atoms are included as C. A $CHCl_3$ molecule is located between the four CH_2CH_2Ph groups attached to each hemisphere. Six other $CHCl_3$ molecules (per host molecule) are located between the hemicarceplexes. Four of these are badly disordered. The two cavitand moieties are not slipped, but are eclipsed with respect to each other (see Chart 2). The planes through the four bridge oxygen atoms of the cavitand moiety (planar within 0.04(1) Å) are 2.90 Å apart, and the angles between normals to these planes and the guest plane are 90°.

The crystal structure of **16**⊙DMSO∪2$C_6H_5NO_2$, crystallized from CH_2Cl_2−C_2H_5OH−$C_6H_5NO_2$, space group $P\bar{1}$, a = 12.984(4) Å, b = 14.664(4) Å, c = 20.454(6) Å, α = 68.501-(6)°, β = 73.722(6)°, γ = 65.177(5)°, V = 3252 Å^3, Z = 1, 6676 unique reflections, 2717 with $I > 2\sigma(I)$, $2\theta_{max} = 100°$, was refined to $R = 0.11$. The host is centrosymmetric, and the DMSO guest is disordered over two sites related by the center of symmetry in the host cavity. One molecule of $C_6H_5NO_2$ is located between the four *n*-pentyl groups attached to each hemisphere. The four bridge oxygen atoms in each cavitand moiety are coplanar within 0.22(1) Å and form a rhombus rather than a square (see Chart 2). These two least-squares oxygen planes are parallel, are 3.73 Å apart, and are shifted about 1.4 Å with respect to one another. No atoms have been refined anisotropically. Disorder in the region of the *n*-pentyl groups has been modeled with partial-occupancy atoms.

Supporting Information Available: Tables of crystallographic data, atomic coordinates and displacement parameters, and bond lengths, bond angles, and torsion angles for each of the five crystal structures (46 pp). This material is contained in many libraries on microfiche, immediately follows this article in the microfilm version of the journal, can be ordered from the ACS, and can be downloaded from the Internet; see any current masthead page for ordering information and Internet access instructions.

JA9602152